The Canadian Mineralogist
Vol. 35, pp. 1069-1091 (1997)

METAMORPHISM IN THE NORTHERN TALTSON MAGMATIC ZONE, NORTHWEST TERRITORIES*

ROBERT G. BERMAN[1] AND HEWITT H. BOSTOCK

Continental Geoscience Division, Geological Survey of Canada, 601 Booth Street, Ottawa, Ontario K1A 0E8

Abstract

The Taltson Magmatic Zone (TMZ) forms the southern part of the Thelon–Taltson orogen, in the Northwest Territories. It is separated from its northern continuation by the Great Slave Lake shear zone – Mcdonald fault zone, a major transform-fault system along which the Slave Province indented the Churchill Province. Within the TMZ, fine-grained metasedimentary and minor mafic volcanic rocks of the Rutledge River Basin (~2.3–2.1 Ga) postdate mixed gneisses and plutonic rocks (largely 2.4–2.3 Ga) that form the Churchill Province to the east. These metasedimentary rocks have been intruded by three Taltson batholiths: the Deskenatlata granodiorite (1.99 Ga), the S-type, Slave monzogranite (1.96 Ga), and the S-type, Konth syenogranite (1.94 Ga). Widespread occurrence of orthopyroxene and the assemblage garnet – cordierite – K-feldspar indicates granulite-facies conditions during emplacement of the Slave and Konth plutons, whereas the Deskanatlata plutonism was accompanied by lower temperatures. Garnet–orthopyroxene thermometry based on the equilibrium: Alm = 3 Fs + Al_2O_3 (in orthopyroxene) yields near-peak temperatures between 920 and 1045°C for most granite and paragneiss samples, whereas recorded pressures are roughly constant at 6.9 ± 0.9 kbar. The distribution of samples with spinel and quartz in contact is centered on the Konth granite, suggesting an increasing thermal regime from ~1.99 to 1.93 Ga, with the highest temperatures reached during the generation and emplacement of the Konth granite. Temperatures recorded by TMZ samples exceed those predicted in published thermal models of thickened continental crust, and appear to be higher than those attending metamorphism in the Thelon orogen. A possible mechanism to account for elevated thermal conditions is increased flux of mantle heat resulting from ocean-ridge subduction following subduction of oceanic crust that produced the Deskenatlata plutonic suite.

Keywords: Taltson Magmatic Zone, geothermobarometry, metamorphism, granulite facies, Al-in-orthopyroxene geothermometer, granitic batholiths of S type, Northwest Territories.

Sommaire

La zone magmatique de Taltson forme la bordure sud de la ceinture orogénique de Thelon–Taltson, dans les Territoires du Nord-Ouest. Elle est séparée de son prolongement vers le nord par un système important de failles transformantes, la zone de cisaillement du Grand Lac de l'Esclave et la faille de Mcdonald, le long de laquelle la Province de l'Esclave a produit une indentation dans la Province de Churchill. Dans cette zone magmatique, des roches métasédimentaires à grains fins et des intercalations de roches métavolcaniques mafiques du bassin de la rivière Rutledge (~2.3–2.1 Ga) sont plus jeunes qu'un cortège mixte de gneiss et de roches plutoniques (en majorité 2.4–2.3 Ga) qui composent la Province de Churchill vers l'est. Ces roches métasédimentaires sont recoupées par trois batholithes de la suite Taltson: la granodiorite de Deskenatlata (1.99 Ga), le monzogranite de type S (1.96 Ga), le syénogranite de Konth, aussi de type S (1.94 Ga). La présence répandue d'orthopyroxene et de l'assemblage grenat – cordiérite – feldspath potassique indique des conditions typiques du faciès granulite au cours de la mise en place des plutons Slave et Konth; en revanche, la mise en place du pluton de Deskanatlata était accompagnée par une température plus faible. Le géothermomètre grenat–orthopyroxène, fondé sur l'équilibre Alm = 3 Fs + Al_2O_3 (dans l'orthopyroxène), donne des températures proches de celles du paroxysme métamorphique, entre 920 et 1045°C, pour la plupart des échantillons de granite et de paragneiss, tandis que les pressions indiquées semblent assez constantes, 6.9 ± 0.9 kbar. La distribution d'échantillons contenant spinelle et quartz en contact est centrée sur le granite de Konth, ce qui fait penser à un régime thermique en croissance entre ~1.99 to 1.93 Ga, la température la plus élevée accompagnant la génération et la mise en place de ce granite. Les températures enregistrées dans les échantillons de cette zone magmatique dépassent celles que prédisent les modèles établis pour une croûte continentale épaissie, et semblent plus élevées que les températures de métamorphisme dans la ceinture orogénique de Thelon. Un mécanisme possible impliquerait un flux de chaleur mantellique accru à cause de la subduction d'une ride océanique suite à la subduction de croûte océanique qui a mené à la formation de la suite plutonique de Deskenatlata.

Mots-clés: zone magmatique de Taltson, géothermobarométrie, métamorphisme, faciès granulite, géothermomètre "Al dans l'orthopyroxène", batholithes granitiques de type S, Territoires du Nord-Ouest.

---

* Geological Survey of Canada contribution number 1997119.
[1] *E-mail address*: berman@gsc.nrcan.gc.ca

Introduction

The Taltson Magmatic Zone (TMZ) consists of a belt of predominantly granitic plutonic rocks of 1.99–1.91 Ga age that extends southward along the western edge of the exposed margin of the Canadian Precambrian Shield from Great Slave Lake shear zone, immediately southeast of Great Slave Lake, to its passage beneath the Paleozoic overlap in northeastern Alberta (Fig. 1). Similar plutonic rocks of the Thelon Orogen extend north from Great Slave Lake shear zone to Prince of Wales Island, forming an overall strike-length of approximately 2550 km for this Early Proterozoic magmatic arc (Hoffman 1988). Nd isotopic signatures and geochemistry of the three main TMZ granite suites (Thériault 1992) support the view that they represent pre-collisional continental arc and continent–continent collisional granites, similar to that proposed for their Thelon Orogen counterparts (Hoffman 1988).

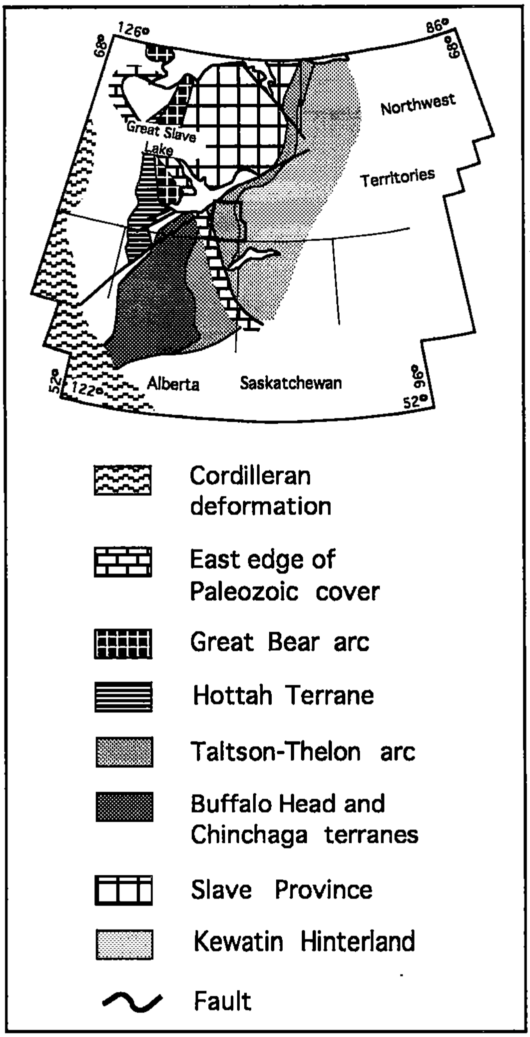

FIG. 1. Regional tectonic map of northwestern North America (after Hoffman 1988).

Previous study of the metamorphic evolution of the TMZ in northeastern Alberta suggested a polyphase metamorphic history with Archean high-P – high-T (900 ± 100°C and 7.5 kbar) granulite-facies metamorphism, followed by ~1.9 Ga lower-P – lower-T granulite-facies ($M_{2.1}$), amphibolite-facies ($M_{2.2}$) and greenschist-facies ($M_{2.3}$) metamorphism (Nielsen *et al.* 1981). North of 60°N, there has been little analysis of the metamorphic history. The purpose of this paper is to fill this gap; we address the question of a polyphase metamorphic history, characterize the P–T conditions associated within the TMZ using a new thermometer involving the Al content of orthopyroxene (Aranovich & Berman 1997) that offers some resolution to the problem of retrograde Fe–Mg exchange in granulites (Fitzsimons & Harley 1994, Pattison & Bégin 1994), and explore some tectonic implications. Lastly, as metamorphic conditions in the TMZ appear to have exceeded the closure temperature of monazite (Heaman & Parrish 1991), the regional geothermometry results can be used to constrain interpretations of new results on geochronology for this part of the TMZ (Bostock & van Breemen, in prep.).

Regional Geology

General description

The TMZ consists primarily of an eastern pair of high-temperature, S-type granitic batholiths flanked on the west by a somewhat older, less aluminous batholith. The eastern batholiths contain enclaves of high-grade paragneiss, interpreted to represent remnants of the Paleoproterozoic Rutledge River basin (Bostock & van Breemen 1994). Sedimentation in this basin is considered to have ended by 2.13–2.09 Ga, the age of some metamorphic overgrowths on zircon, and of monazite in the Rutledge River paragneiss (Bostock & van Breemen 1994).

The TMZ lies at the western margin of an extensive region of older gneisses and plutonic rocks comprising the Rae Province (Figs. 2, 3). The two regions are separated by a complex, polydeformational, predominantly sinistral strike-slip, ductile–brittle shear zone (the East Boundary shear zone), which deformed the margins of both regions during and after the Taltson episode of plutonism. Early movements along this zone are reflected in a broad halo of variably foliated and retrograded gneisses, whereas later movements were concentrated along more discrete zones of mylonite, which divide the East Boundary shear zone into major blocks. The westernmost continuous mylonites, the Allan and Gagnon shear zones, are used here to define the boundary between the TMZ and Rae Province (Fig.

3), although sediments of the Rutledge River basin may have overlapped this boundary eastward, and lesser plutons of Taltson age have intruded rocks to the east.

The Rae Province

The oldest rocks along the western margin of the Rae Province are granitoid gneisses, which include variously altered and contaminated amphibolitic dykes, layers, and lenses of unknown age. Granitic phases from these gneisses in the northern TMZ (north of the 60th parallel) have yielded U–Pb zircon ages in the range 2.44–2.27 Ga (Bostock & Loveridge 1988, Bostock *et al.* 1991), with some indication of Archean inheritance. Undated, tectonized remnants of high-grade pelitic to quartzitic paragneiss are present in the southern fault blocks, and a tectonically isolated remnant of greenschist-facies greywacke–mudstone is present at Hill Island Lake (Mulligan & Taylor 1969, Bostock 1984, 1992). In terms of geochronological constraints, the protoliths for these metasedimentary rocks could be Rutledge River basin sediments (Bostock & van Breemen 1994). Unmetamorphosed Nonacho Group conglomerates (Aspler & Donaldson 1986) were unconformably deposited after 2.06 Ga (van Breemen & Aspler 1994), but probably before 1.906 Ga, a local minimum age for sinistral shear widely evident within the group (Bostock & Loveridge 1988).

The Taltson Magmatic Zone

The Deskenatlata Granodiorite complex (Fig. 2), dated by U–Pb zircon geochronology at 1.986 ± 0.02 Ga (Bostock *et al.* 1987), varies from hornblende diorite to granite in composition and from medium or fine grained to coarse grained or megacrystic in texture. Hornblende, biotite or chlorite may be the dominant mafic mineral. No orthopyroxene has been found in the granodiorite, but orthopyroxene is present in some mafic inclusions within it. K-feldspar is characteristically perthitic microcline. Granodiorite near the eastern boundary of the complex locally contains monazite in association with remnants of Rutledge River paragneiss.

The mostly medium-grained, equigranular, S-type, monzogranitic Slave batholith is widely garnet–cordierite–spinel-bearing, and locally contains orthopyroxene. Accessory minerals include monazite, ilmenite, zircon and, locally, apatite. K-feldspar varies from perthitic microcline to mesoperthite in different areas. The Slave batholith has been dated just south of the Great Slave Lake shear zone at 1.96 Ga (no errors quoted) using zircon (Hanmer *et al.* 1992), and just south of the sixty-first parallel at 1.955 ± 0.002 Ga using monazite (Bostock *et al.* 1987).

The younger of the peraluminous, S-type TMZ batholiths is the Konth megacrystic syenogranite (1.94 Ga based on monazite: Bostock *et al.* 1987, Bostock & Loveridge 1988) emplaced largely along the central axis and east margin of the Slave granite. Its major mineralogy is like that of the Slave batholith, except that K-feldspar is variably megacrystic, commonly with crystals up to 2 cm or more in length, and medium-grained plagioclase is less common. The megacrysts are typically, and matrix K-feldspar is locally, mesoperthitic to submesoperthitic, in contrast to K-feldspar in the Deskenatlata and most parts of the Slave batholith.

The Konth batholith is separated from the petrographically similar Arch Lake granite by a line of discontinuous screens of paragneiss that runs diagonally from Rutledge Lake through Pilot Lake and into Alberta, such that the greater part of the Arch Lake granite occurs in Alberta (Godfrey & Langenberg 1978, McDonough *et al.* 1995), and only a long northward-tapering wedge is present in the northern TMZ (Fig. 2). Whereas the Konth contains remnants of quartz-rich to pelitic paragneiss, inclusions of widely varying size and proportion (Fig. 2), and the peraluminous minerals garnet, cordierite, and spinel, these features are largely absent in the Arch Lake granite. Slave-like remnants do, however, occur in both the Konth and Arch Lake granites. Inasmuch as these two granites have major petrographic similarities (both are monazite-bearing, K-feldspar megacrystic syenogranites), they are likely related both structurally and petrogenetically. The Arch Lake granite has been dated at 1.938 ± 0.003 Ga (zircon: V.I. McNicoll, pers. commun., 1996) and *ca.* 1.935 Ga (monazite: Bostock & van Breemen, in prep.), whereas monazite in the Konth granite yields ages of 1.938 ± 0.003 and 1.935 ± 0.003 Ga (Bostock & Loveridge 1988). These ages do not preclude the possibility that the Arch Lake granite is slightly younger than the Konth, as suggested by apparent cross-cutting of the Konth aeromagnetic trend by that of the Arch Lake near Pilot Lake. The granite that crosses Gagnon Lake east of the Gagnon shear zone is mineralogically and texturally diverse, but is tentatively correlated with the Arch Lake granite on the basis of similar monazite ages and the presence of megacrystic phases along its western and northwestern margin.

Late Taltson granites (Natael, Othikethe Falls, Benna Thy) are smaller plutons that were intruded in the interval from 1.934 to 1.906 Ga. They are mostly equigranular, foliated, late-syntectonic bodies emplaced within or adjacent to the marginal shear zones that surround the S-type granites of northern TMZ. Minor syntectonic dykes of muscovite-bearing granite (not shown on Fig. 2) and pegmatites intrude the paragneiss of Rutledge River basin at Thubun Lakes. Although these have not been directly dated, two crystals of monazite and a single near-concordant crystal of zircon from the local paragneiss give ages of between 1.904 and 1.907 Ga, interpreted as the age of metamorphism

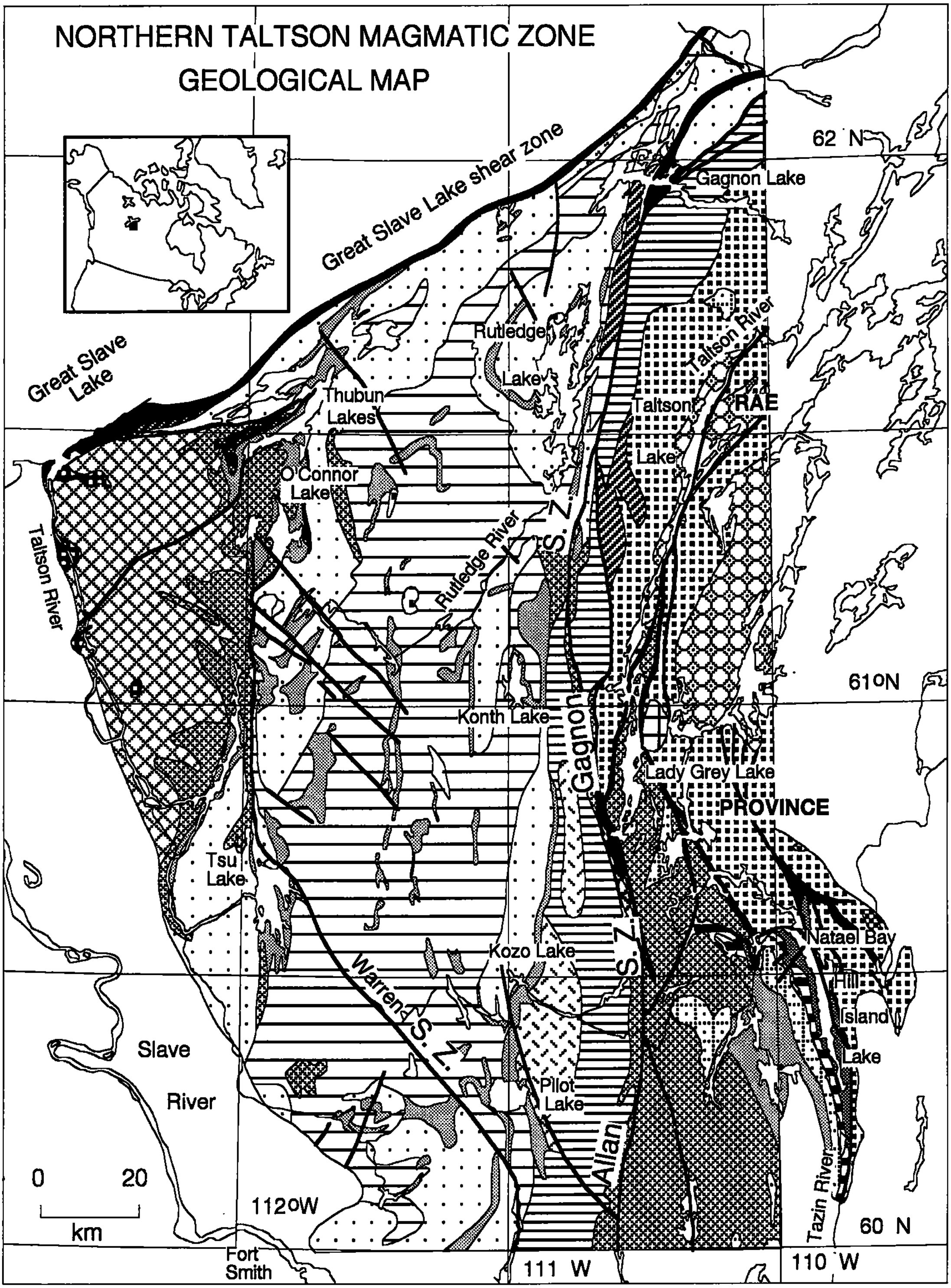
NORTHERN TALTSON MAGMATIC ZONE
GEOLOGICAL MAP
Great Slave Lake shear zone
Great Slave Lake
Thubun Lakes
O'Connor Lake
Rutledge Lake
Gagnon Lake
Taltson River
Taltson Lake
RAE
PROVINCE
Rutledge River
S. Z.
Gagnon
Konth Lake
Lady Grey Lake
Tsu Lake
Kozo Lake
Warren S. Z.
Allan S. Z.
Pilot Lake
Natael Bay
Hill Island Lake
Tazin River
Slave River
Fort Smith
0 20 km
62 N
61ON
60 N
112OW
111 W
110 W

that accompanied emplacement of these bodies (Bostock & van Breemen 1994).

Remnants of tonalitic gneiss and mafic inclusions of Archean age (Burwash *et al.* 1985, McDonough *et al.* 1995) have been found in Alberta, but the Rutledge River paragneiss forms the most abundant enclaves, ranging up to ~50 km in length (paragneiss of Fig. 2). These rocks consist mostly of semipelitic to pelitic, locally graphite-bearing gneisses with common quartz-rich gneiss horizons (paragneiss of Fig. 2). Calc-silicate layers and amphibolite are found locally, and marble is rare. Widespread within the Rutledge River paragneiss remnants are bands, up to 100 m thick and ~1 km in length, of plagioclase – quartz – orthopyroxene ± K-feldspar ± garnet ± biotite gneiss that constitutes the source of many of the samples analyzed in the present study. Also forming remnants within the S-type batholiths are at least three bodies, mappable at a scale of 1:250,000, of medium-grained plagioclase – quartz – orthopyroxene charnockites with variable contents of K-feldspar and biotite. The age of these is unknown.

In addition to remnants of Rutledge River paragneiss, the Slave batholith contains a minor (<1%), widely scattered component of medium-grained, pyroxene-bearing, anorthositic to ultramafic rocks. Most of these bodies are small (<10 m) and appear to be included within the granite. Two larger bodies are potentially correlative with the Slave batholith. The undated Tsu Lake metagabbro forms a 1 km by 3 km, chevron-shaped lens associated with mixed gneisses within the Slave batholith west of Tsu Lake (Fig. 2). A minimally deformed layer of metaleucogabbro of unknown thickness occurs within mafic gneisses southeast of Rutledge Lake along the western margin of Rae Province (Fig. 2). Crystals of zircon from an anorthosite layer give an upper intercept age of 1956 ± 3 Ma (Bostock *et al.* 1991), interpreted as its age of emplacement, coeval with the Slave batholith.

Foliation trends within Konth batholith and its immediately adjacent country-rocks tend to reflect the trends of the nearest contacts (Fig. 3), with exceptions in two regions. Southwest of Warren fault zone, foliations are extensively subhorizontal, and the granite may form a major sill or uplifted floor region of the Konth magma chamber. Near the northern margin of the Konth batholith, foliations suggest an interplay of northerly trends parallel to the east and west walls of the intrusion and northeasterly trends parallel to Great Slave Lake shear zone. Dips associated with the northeasterly trends are commonly moderate to shallow southeastward within the Konth batholith, but steepen progressively through the Slave granite to vertical within the mylonites of Great Slave Lake shear zone. This pattern is interpreted to reflect a dynamic equilibrium between periods of active transpression along Great Slave Lake shear zone and emplacement of the Konth granite. The chronological constraints for ductile movement along the Great Slave Lake shear zone (2.0–1.9 Ga, Hanmer *et al.* 1992) and for emplacement of the Konth batholith (~1.94 Ga, Bostock & van Breemen, in prep.) support this interpretation.

Regional Metamorphism of the Taltson Magmatic Zone

Observed mineral assemblages (Fig. 4) indicate that maximum temperatures associated with the peraluminous Slave and Konth granites appear to

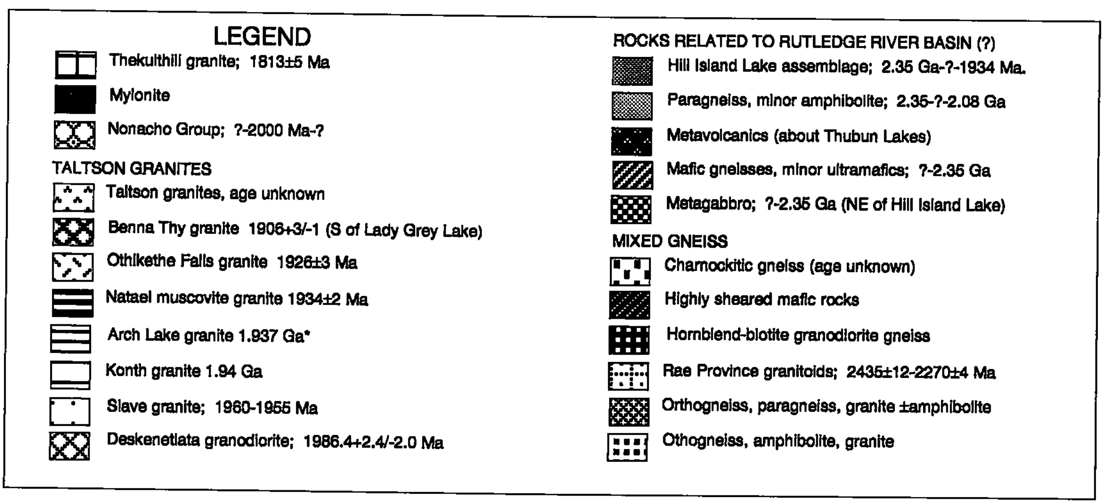

FIG. 2. Simplified geological map of the northern Taltson Magmatic Zone.

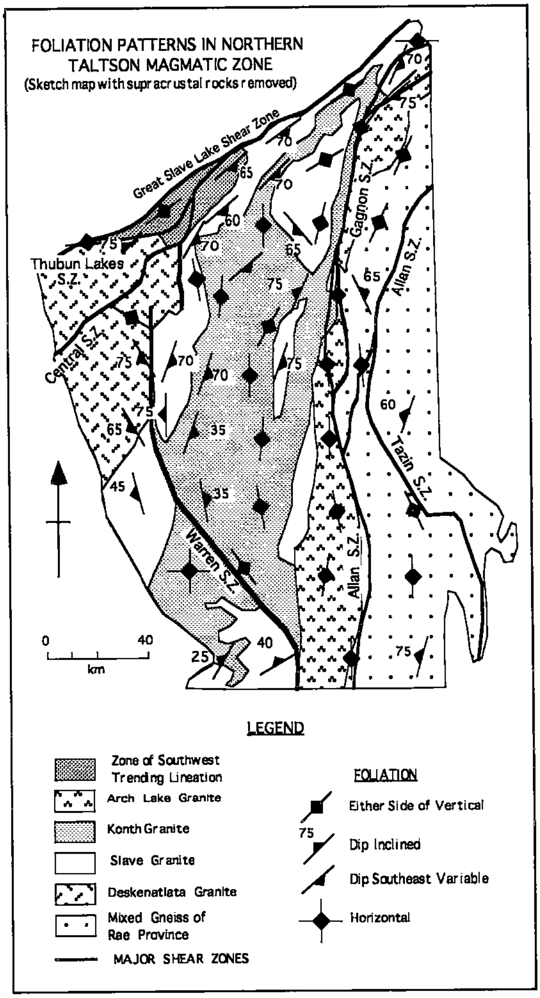

FIG. 3. Foliation trends within the northern Taltson Magmatic Zone. Note the presence of Rae Province gneisses east of the Allan shear zone.

have been broadly similar, and higher than those associated with the Deskenatlata granite. Metamorphic orthopyroxene is widespread in metagabbro and paragneiss enclaves within the Slave and Konth batholiths (Fig. 4a). The Slave and Konth granites also locally contain igneous orthopyroxene, whereas the Deskenatlata complex contains only rare orthopyroxene-bearing inclusions. Mesoperthite, common in granulite-facies rocks and large deep-seated intrusions (Smith & Brown 1988), is widespread in the Slave and Konth granites, but does not occur in the Deskenatlata granite (Fig. 4b). The general attainment of transitional upper-amphibolite- to granulite-facies conditions is indicated by the abundance in paragneiss of Grt–Crd–Kfs assemblages (Fig. 4c) stable on the high-temperature side of the model KFMASH reaction (Fig. 5):

$$\mathrm{Bt + Sil + Qtz = Grt + Crd + Kfs + H_2O} \qquad (1)$$

The greater abundance of the six-phase assemblage corresponding to reaction (1) in areas along the margins of the Konth and Slave batholiths (Fig. 4c) suggests retrograde operation of this reaction due to fluid access along these margins.

The occurrence of quartz and spinel in contact provides evidence of high-temperature granulite conditions (≥~ 800°C: Waters 1991), although this assemblage can be stable in iron-rich bulk compositions at somewhat lower temperature (Xu *et al.* 1994). Spinel-bearing assemblages within granitic rocks and rafts of paragneiss are present in most parts of the Konth granite. The two minerals are in minimally to moderately altered contact over most of the central and western part of the Konth granite (Fig. 4d), but contacts tend to be more altered or absent along its eastern margin, suggesting somewhat lower temperatures, combined with more advanced retrogression along this margin. Orthopyroxene – spinel – quartz, indicative of higher temperatures than spinel – quartz (Hensen & Green 1973), occurs in just one sample of paragneiss northeast of Tsu Lake.

Temperatures reported below appear to have been locally sufficiently high (~950°C: Audibert *et al.* 1995) to stablilize osumilite. Its absence in TMZ gneisses is likely due to the more Mg-rich bulk compositions required to stabilize osumilite (*e.g.*, Waters 1991). Neither kyanite (except for a single occurrence reported from tectonic inclusions in gneiss of the Pilot Lake area (Burwash & Cape 1981) nor Opx–Sil–Qtz-bearing assemblages have been found. The latter assemblage constrains TMZ pressures to less than about 9.5 kbar at 900°C (Fig. 5; Carrington 1995, Aranovich & Berman 1996).

SUMMARY OF PETROGRAPHY

The following summary of the main petrographic features of TMZ samples is based on observation of approximately 3000 thin sections.

The Slave and Konth are peraluminous granites with similar mineralogy. The Konth is distinguished by abundant K-feldspar megacrysts, up to 2 cm in length, forming sutured grain-boundaries with finer-grained (~0.5–1 mm) matrix feldspars and quartz. Primary biotite forms rare, interstitial grains suggesting high-temperature, low-$a(H_2O)$ melting conditions similar to those applicable to A-type granites (*e.g.*, Landenberger & Collins 1996). Greater modal abundance of biotite in the Slave granite suggest formation at somewhat lower temperature or higher $a(H_2O)$. Anhedral, nonpoikilitic garnet (<6 mm) and orthopyroxene (0.2–8 mm) are generally separated by

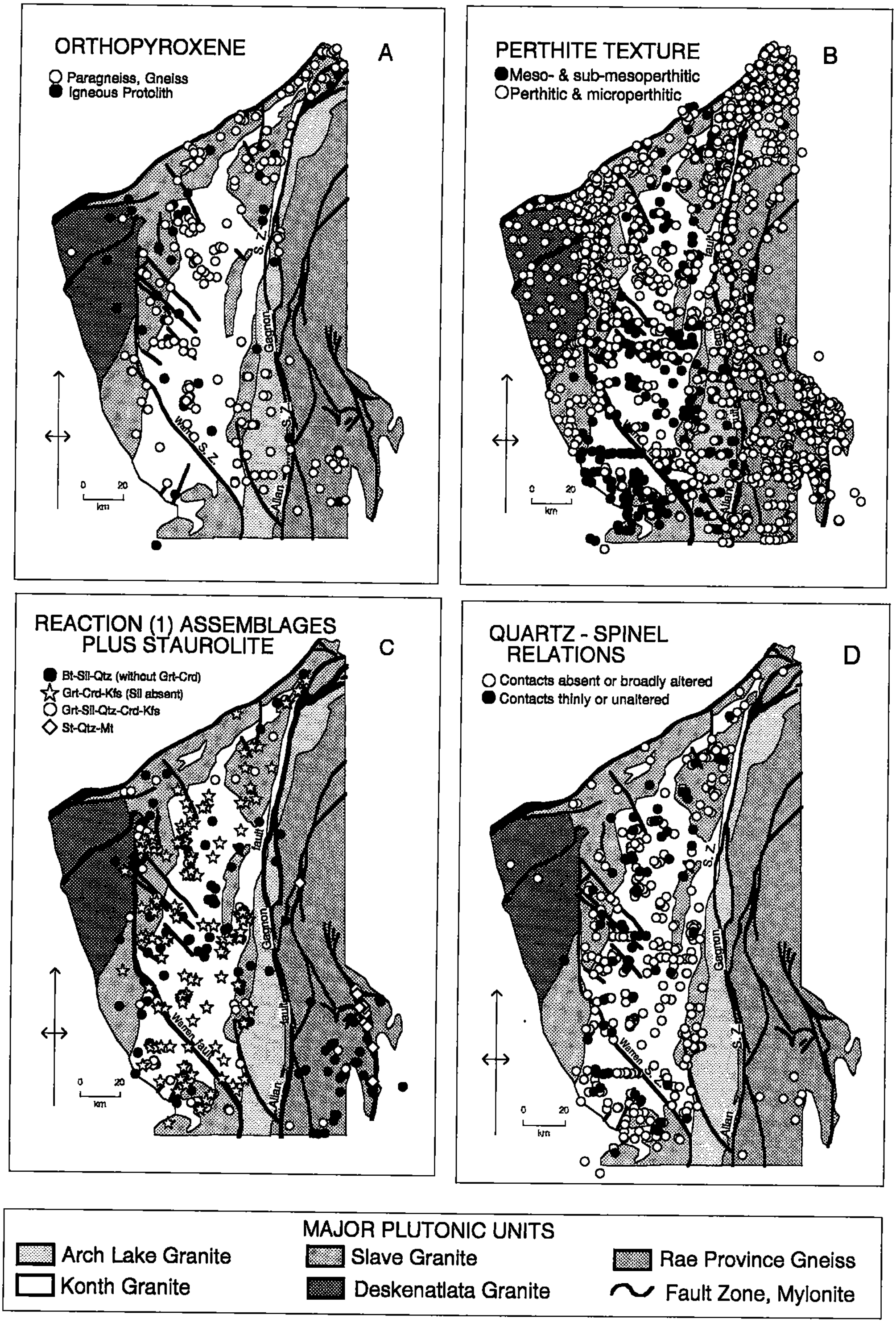

FIG. 4. Regional distribution of (a) orthopyroxene, (b) perthitic feldspar, (c) subassemblages of reaction (1) and staurolite, (d) spinel + quartz.

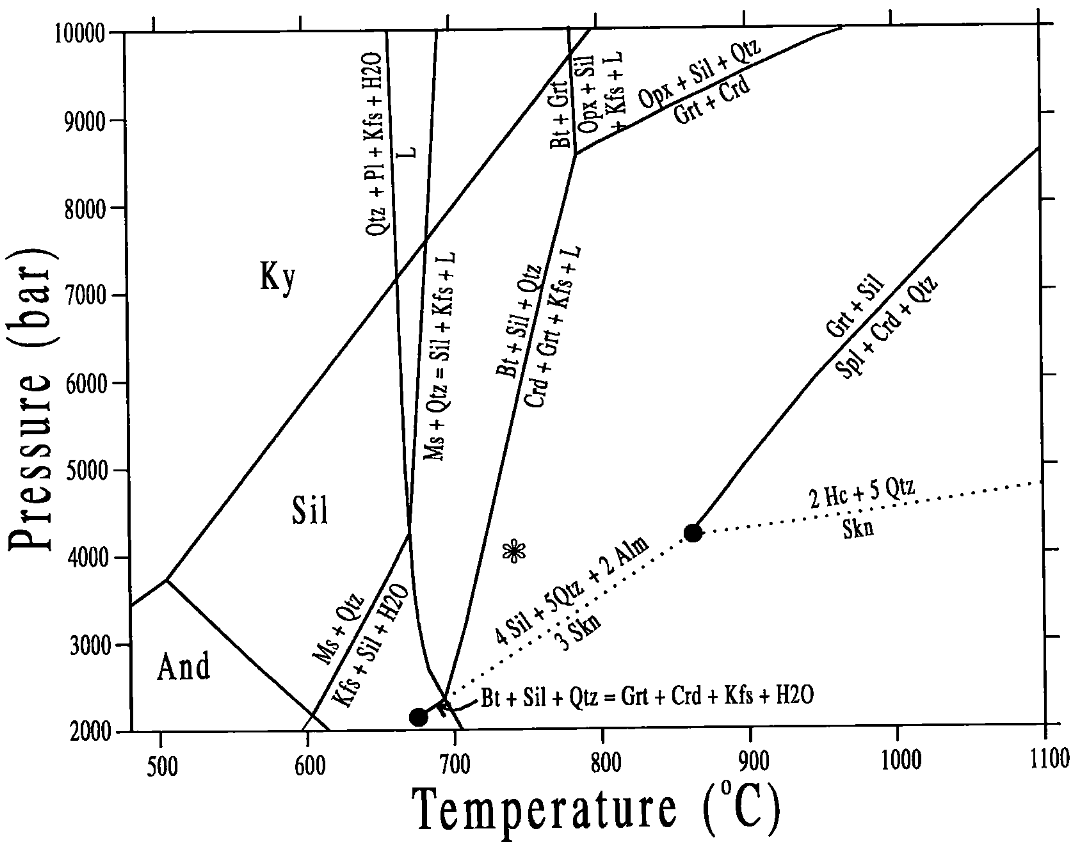

FIG. 5. Reactions in the KFMASH petrogenetic grid computed with THERIAK (de Capitani & Brown 1987) using thermodynamic data of Berman & Aranovich (in prep.). Solid curves involve Fe–Mg minerals of changing composition. Filled circles are singular points at which the garnet becomes pure almandine. Dotted curves are FAS equilibria. Melt (L) curves from Davidson *et al.* (1990). The reaction Grt + Sil = Spl + Crd + Qtz (5) shifts to lower temperature in response to the presence of Zn and Fe^{3+} (Waters 1991), toward the position of the invariant point (asterisk), as estimated by Fitzsimons (1996). Skn represents sekaninaite, the Fe end-member of cordierite.

quartz, plagioclase, and K-feldspar. Where they are in contact, reaction relations are generally absent, but some samples contain partial coronae of garnet around orthopyroxene (Fig. 6a), suggesting cooling through the model continuous reaction:

$$\text{Grt} + \text{Qtz} = \text{Opx} + \text{Pl} \tag{2}$$

Garnet more commonly forms grains isolated from other ferromagnesian minerals or complete coronae around ilmenite adjacent to plagioclase and quartz (Fig. 6b). Minor biotite occurs as partial, late rims on some orthopyroxene and garnet grains. Small (<0.5 mm), anhedral grains of spinel occur isolated, in contact with matrix feldspar or completely surrounded by cordierite, up to 5 mm in size, that is adjacent to quartz. The latter relationship suggests that this cordierite may have formed during emplacement of the granites at higher levels in the crust *via* the pressure-sensitive FAS model reaction (Fig. 5):

$$2\ \text{Hc} + 5\ \text{Qtz} = \text{Skn} \tag{3}$$

Paragneiss samples contain two different mineral assemblages with no regular spatial distribution: Grt – Opx – Bt – Pl – Qtz – Kfs – Ilm ± Spl, Crd, and Grt – Crd – Bt – Pl – Qtz – Kfs – Ilm ± Sil, Spl, Crn, And (Table 1). The main mineralogical differences can be accounted for by the higher proportion of Al in the bulk composition of the latter assemblage.

In Grt–Opx paragneisses, orthopyroxene and garnet commonly occur as separate, thin layers in a matrix of moderately flattened (aspect ratio between 2 and 5:1) quartz and feldspar, together with minor biotite. Orthopyroxene occurs as anhedral grains between 0.2 and 15 mm, in places partially altered to

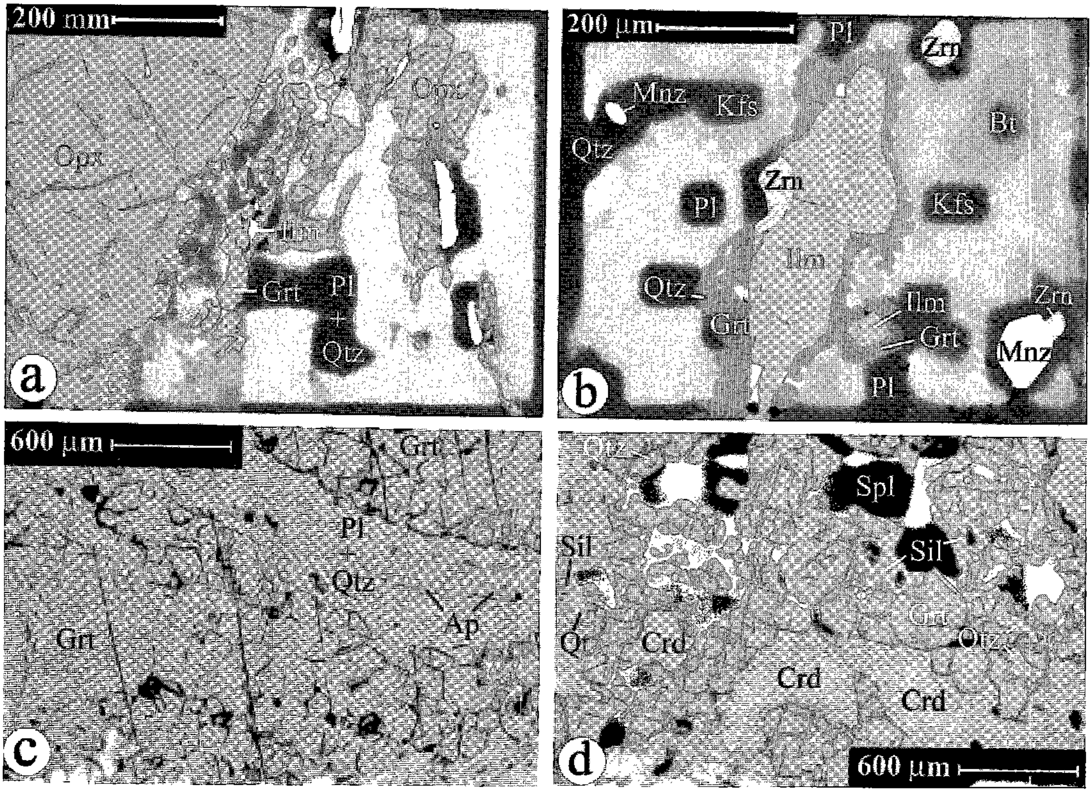

FIG. 6. Back-scattered SEM image for sample 718a, showing (a) corona of garnet around orthopyroxene, and (b) ilmenite. Plane-polarized photomicrographs illustrate (c) protomylonite in sample 505B, and (d) formation of Grt–Sil from Crd–Spl–Qtz in sample 780A.

a serpentine-group mineral. Rarely orthopyroxene is rimmed by a symplectitic intergrowth of biotite and quartz, suggesting late breakdown of orthopyroxene *via* the continuous KFMASH model reaction:

$$\text{Bt} + \text{Qtz} = \text{Opx} + \text{Kfs} + H_2O \quad (4)$$

Modal proportions of biotite and orthopyroxene vary antithetically among various samples, which is suggestive of local variations in activity of H_2O or bulk Fe/(Fe + Mg). Garnet forms highly irregular, lobate grains, with inclusions of quartz and biotite, as well as partial rims around orthopyroxene adjacent to plagioclase and quartz (similar to that shown in Fig. 6a). In some samples, garnet occurs as inclusions surrounded by a moat of plagioclase within large grains of orthopyroxene, suggesting a clockwise P–T path, with early crystallization of garnet, followed by heating or decompression to form Opx + Pl *via* model reaction (2).

In all samples, garnet and orthopyroxene formed early with respect to the dominant foliation, which in samples proximal to lithological contacts or shear zones is protomylonitic (Fig. 6c). This observation indicates that these shear zones, which have been interpreted as forming southward escape-structures accommodating indentation of the Slave into the Rae Province (Gibb 1978, Hanmer *et al.* 1992, McDonough *et al.* 1995), remained active after cessation of TMZ magmatism. That they formed at the granulite grade is suggested by textural evidence of feldspar deformation textures (McDonough *et al.* 1995) and demonstrated by the essentially identical chemistry of garnet porphyroblasts and recrystallized garnet within protomylonites (Fig. 6c).

Grt–Crd paragneisses have granoblastic textures with sutured grain-boundaries among cordierite, K-feldspar, quartz, and plagioclase. Sillimanite occurs as porphyroblasts up to 1 cm, and smaller grains associated with anhedral, irregularly shaped garnet that commonly includes isolated, rounded grains of spinel, cordierite and quartz. The silimanite, which varies among samples from coarse to fibrolitic, also encloses embayed or anhedral spinel (some with small, round

TABLE 1. TALTSON MAGMATIC ZONE SAMPLE LOCATIONS AND ASSEMBLAGES

Sample	*Lithology*	*Easting*	*Northing*	*Grt*	*Opx*	*Crd*	*Bt*	*Spl*	*Sil*	*And*	*Qtz*	*Pl*	*Kfs*	*Ms*	*Crn*
87BKM-258A	K	481920	6785220	x	x	-	x	x	-	-	x	x	x	-	-
80BKD-353A	K	478430	6716000	x	x	-	x	-	-	-	x	x	x	-	-
87BKM-317A	K	468010	6810400	x	x	-	x	-	-	-	x	x	x	-	-
80BK-718A	K	498410	6679760	x	x	-	x	-	-	-	x	x	x	-	-
80BKC-2063	S	473100	6719780	x	x	x	x	x	-	-	x	x	x	-	-
80BK-879A	S	482260	6664340	x	-	x	x	x	-	x	x	-	x	-	x
80BKD-310A	P-K	489380	6730960	x	x	-	x	x	-	-	x	x	-	-	-
85BKJ-96B	P-K	476410	6791170	x	x	x	x	-	-	-	x	x	x	-	-
80BK-484A	P-K	484520	6699000	x	-	x	x	x	-	x	x	x	-	x	x
85BKJ-229B	P-K	474350	6780020	x	-	x	x	x	-	x	x	x	x	-	x
89BK-111A	P-K	484480	6816060	x	-	x	x	x	x	-	-	-	x	-	-
83BKJ-760A	P-K	502730	6765190	x	-	x	x	x	-	x	x	x	-	x	x
83BKJ-736A	P-K	502590	6763250	x	-	x	x	x	-	-	x	-	x	-	-
87BKO-59B	P-S	467420	6831390	x	x	-	x	-	-	-	x	x	-	-	-
87BKN-145B	P-S	496600	6828900	x	x	-	x	-	-	-	x	x	x	-	-
86BKL-40A	P-S	464820	6774400	x	x	x	x	x	-	-	x	x	-	-	-
87BKO-505B	P-S	512040	6849980	x	x	-	x	x	-	-	x	x	x	-	-
87BKO-223B	P-S	498050	6863100	x	x	x	x	-	-	-	x	x .	x	x	-
86BKJ-106B	P-S	477210	6792800	x	x	-	x	-	-	-	x	x	x	-	-
87BKO-187C	P-S	499100	6862300	x	x	-	x	-	-	-	x	x	x	x	-
88BK-127A	P-S	478270	6851580	x	-	x	x	x	x	-	x	x	x	-	-
80BKD-493A	P-S	497020	6663520	x	-	x	x	x	x	-	x	-	x	-	-
86BKL-30A	P-S	457790	6787500	x	-	x	x	-	x	-	x	x	-	x	-
89BK-96A	P-S	450800	6784530	x	-	x	x		x	-	x	x	x	x	-
87BKL-403A	P-S	503870	6818500	x	-	x	x	x	x	-	-	-	-	-	-
86BKL-387C	P-S	508800	6820420	x	-	x	x		-	-	x	x	x	x	-
87BKN-105A	P-S	500800	6843050	x	-	x	x	x	x	x	x	x	-	x	-
80BK-880A	P-S	482210	6664680	x	-	x	x	x	-	x	x	-	x	-	x
91BK-19A	P-S	544460	6888260	x	-	x	x	x	x	-	-	-	x	-	-
79BKA-780A	P-KS	451400	6716320	x	-	x	x	x	x	-	x	-	x	x	-
80BK-797A	P-KS	472390	6679400	x	-	x	x	x	-	-	-	x	x	-	-
81BKG-59A	P-R	547100	6669600	x	x	-	x	-	-	-	x	x	-	-	-

K: Konth granite, S: Slave granite; P–K, P–S, P–R, P–KS: paragneiss within Konth, Slave, Rae Province, and Konth-Slave contact, respectively.

inclusions of quartz), and is itself partly enclosed by or intergrown with garnet. These textures (Fig. 6d) suggest late formation of Grt + Sil during cooling through a model reaction that can be written as (Fig. 5; Clarke & Powell 1991, Waters 1991, Fitzsimons 1996):

$$\text{Grt} + \text{Sil} = \text{Spl} + \text{Crd} + \text{Qtz} \quad (5)$$

Biotite-rich samples have small, embayed grains of spinel and ragged grains of cordierite surrounded by intergrowths of biotite and sillimanite, also suggesting cooling through the model reaction:

$$\text{Bt} + \text{Sil} + \text{Qtz} = \text{Crd} + \text{Kfs} + \text{Spl} + \text{L} \quad (6),$$

which intersects reaction (5) at an Opx-absent invariant point estimated to be located at approximately 4 kbar and 740°C (Fitzsimons 1996). Low-temperature alteration of spinel is also indicated by relict grains surrounded by corundum associated with muscovite and chlorite. Coarse needles of sillimanite are commonly included in poikiloblastic andalusite that is rimmed by fine aggregates of sillimanite. These textures point to late crystallization of andalusite followed by renewed growth of sillimanite likely related to late reheating at low pressure. Muscovite occurs as late porphyroblasts cross-cutting the foliation defined by aligned grains of biotite and sillimanite, or replacing biotite. Most of the biotite is aligned to form a prominent foliation, but some random orientations and anhedral garnet in some sillimanite-bearing samples completely rimmed by biotite suggest late operation of the model reaction (1).

Previous investigations of metamorphic conditions within the southern TMZ (Nielsen *et al.* 1981, Chacko *et al.* 1994, Chacko & Creaser 1995) have emphasized that paragneiss samples probably represent restite from partial melting of pelitic source-rocks. A major restite component in many paragneiss samples studied here is precluded by their significant modal biotite and quartz, two minerals that are depleted early during biotite dehydration-induced melting (Patiño Douce & Johnston 1991). Spinel- and garnet-rich samples, however, contain up to about 20 modal % spinel and 15% garnet that form irregular, anhedral grains up to 1 mm and 1 cm across, respectively. Both include rounded grains of biotite, K-feldspar, and cordierite, whereas some spinel is completely included by garnet. The matrix consists of cordierite, K-feldspar, and plagioclase, without quartz. The mineralogy of this sample makes it a good candidate for restite produced through high-temperature (~950°C) melting of a pelitic source-rock (Patiño Douce & Johnston 1991).

Mineral Chemistry and Geothermobarometry

Method

Thermal conditions prevailing during evolution of the TMZ have been assessed on the basis of detailed mineral compositions and geothermobarometry for 33 samples. Five of the latter group are samples of the Slave or Konth granite, and 28 are samples of paragneiss collected from enclaves within these granites. Sample locations and observed mineral assemblages are listed in Table 1. Sample sites were chosen to ensure representative coverage of the northern TMZ, dependent on the availability of hand samples collected during 1:250,000 scale mapping and on degree of local retrogression.

Chemical analyses of garnet, cordierite, orthopyroxene, biotite, spinel, and plagioclase were done on standard polished thin sections with a Cameca SX–50 electron microprobe equipped with four wavelength-dispersion spectrometers. The microprobe was operated at 15 kV with beam current of 10 or 30 nA depending on the element, sample stability and size. The raw counts were transformed to concentrations of elements using the Cameca PAP program (Pouchou & Pichoir 1985). Detailed compositional profiles (rim–core–rim) were obtained for minerals (Grt, Opx, Crd, Pl) used in thermobarometry calculations. For each sample, two to four areas containing the required assemblage of minerals were analyzed. Mineral compositions used in geothermobarometry calculations are given in Tables 2–5.

TABLE 2. COMPOSITION OF GARNET, NORTHERN TALTSON MAGMATIC ZONE

Sample	*258A*	*353A*	*317A*	*718A*	*2063A*	*310A*	*96B*	*59B*	*145B*	*40A*	*505B*	*223B*	*106B*	*187C*	*127A*	*30A*	*59A*
FeO	31.60	33.43	29.76	32.54	32.31	33.05	29.80	31.78	29.00	29.76	26.98	30.55	29.90	30.42	35.90	33.34	33.15
MgO	7.12	5.12	8.07	7.01	7.10	6.12	8.73	6.10	7.16	8.20	9.69	8.01	8.70	7.68	4.10	4.98	3.52
SiO2	37.88	37.12	38.27	37.16	36.93	37.51	37.80	37.58	38.01	37.34	38.90	38.46	38.17	38.17	35.99	36.66	36.96
CaO	1.09	1.76	0.96	1.21	0.72	1.32	1.12	1.13	1.25	1.01	1.14	1.08	1.23	1.06	0.61	0.77	3.71
MnO	0.81	0.95	0.75	0.72	0.64	0.62	0.72	0.89	1.79	0.76	0.58	0.53	0.81	0.57	0.95	0.53	1.45
Al2O3	21.10	21.33	21.28	21.80	21.65	21.55	21.20	21.33	21.30	21.24	21.50	21.46	21.95	21.09	20.93	20.69	21.46
TOTAL	99.77	99.71	99.42	100.44	99.36	100.16	99.36	98.81	98.52	98.31	98.95	100.08	100.76	98.99	98.49	97.27	100.40
Fe/(Fe+Mg)	0.714	0.786	0.674	0.723	0.719	0.752	0.657	0.745	0.695	0.671	0.610	0.681	0.658	0.690	0.831	0.790	0.841
Grs	0.030	0.049	0.027	0.033	0.020	0.037	0.030	0.032	0.035	0.028	0.031	0.030	0.033	0.030	0.017	0.023	0.104
Alm	0.680	0.730	0.645	0.688	0.694	0.714	0.627	0.706	0.642	0.641	0.583	0.654	0.625	0.661	0.799	0.762	0.726
Prp	0.273	0.199	0.312	0.264	0.272	0.236	0.327	0.241	0.282	0.315	0.373	0.306	0.324	0.297	0.163	0.203	0.138
Sps	0.018	0.021	0.016	0.015	0.014	0.013	0.015	0.020	0.040	0.017	0.013	0.011	0.017	0.013	0.021	0.012	0.032

Compositions expressed as oxides quoted in wt.%

TABLE 3. COMPOSITION OF ORTHOPYROXENE, NORTHERN TALTSON MAGMATIC ZONE

Sample	*258A*	*353A*	*317A*	*718A*	*2063A*	*310A*	*96B*	*59B*	*145B*	*40A*	*505B*	*223B*	*106B*	*187C*	*59A*
FeO	30.74	31.59	26.60	32.11	31.72	33.20	27.25	30.94	27.32	27.79	24.67	28.64	28.20	28.56	37.37
MgO	14.88	14.93	17.27	15.42	13.79	14.30	17.06	15.19	17.24	16.82	19.25	15.92	17.40	16.69	10.47
SiO2	47.02	47.60	48.21	48.23	45.23	47.20	46.54	48.41	48.75	47.94	49.11	48.41	47.51	47.99	48.18
CaO	0.08	0.23	0.08	0.06	0.09	0.14	0.14	0.16	0.12	0.13	0.11	0.11	0.10	0.09	0.49
MnO	0.29	0.29	0.14	0.24	0.33	0.11	0.24	0.52	0.50	0.29	0.32	0.22	0.15	0.18	0.63
Al2O3	6.16	4.25	6.44	4.61	6.85	4.56	6.54	3.48	4.69	4.74	5.36	5.04	5.49	5.55	1.79
TOTAL	99.60	99.15	99.21	100.93	98.24	99.83	98.39	98.96	98.84	98.08	99.32	98.81	99.28	99.36	99.18
Fe/(Fe+Mg)	0.537	0.543	0.464	0.539	0.563	0.566	0.473	0.533	0.471	0.481	0.418	0.502	0.476	0.490	0.667

Compositions expressed as oxides quoted in wt.%

TABLE 4. COMPOSITION OF PLAGIOCLASE, NORTHERN TALTSON MAGMATIC ZONE

Sample	*258A*	*353A*	*317A*	*718A*	*2063A*	*310A*	*96B*	*59B*	*145B*	*40A*	*505B*	*223B*	*106B*	*187C*	*127A*	*30A*	*59A*
CaO	6.47	8.21	6.65	7.16	4.86	7.20	7.27	6.33	6.07	7.84	7.95	6.94	7.83	5.91	4.53	5.39	7.59
Na2O	8.05	6.79	7.92	7.62	8.51	7.04	7.49	8.10	8.27	7.04	6.79	7.60	7.01	8.28	8.98	8.56	7.30
K2O	0.29	0.15	0.20	0.23	0.56	0.51	0.27	0.32	0.19	0.18	0.45	0.39	0.36	0.32	0.16	0.22	0.20
FeO	0.11	0.11	0.09	0.06	0.08	0.12	0.00	0.05	0.10	0.03	0.12	0.05	0.00	0.07	0.06	0.21	0.06
SiO2	62.14	57.97	61.43	59.84	61.93	59.53	59.52	61.18	62.07	58.25	59.15	60.59	59.06	62.83	63.07	62.31	60.05
Al2O3	24.87	26.37	25.27	25.79	23.65	25.24	25.37	24.40	24.39	25.96	25.66	25.33	26.14	24.32	23.60	24.17	25.63
TOTAL	101.93	99.61	101.56	100.70	99.64	99.67	99.96	100.53	101.10	99.35	100.20	100.90	100.40	101.75	100.40	100.90	100.90
An	0.245	0.303	0.252	0.267	0.197	0.275	0.271	0.240	0.233	0.291	0.295	0.261	0.374	0.228	0.185	0.213	0.281
Ab	0.551	0.454	0.543	0.514	0.623	0.487	0.505	0.557	0.576	0.473	0.456	0.517	0.606	0.579	0.663	0.611	0.490
Or	0.013	0.007	0.009	0.010	0.027	0.023	0.012	0.014	0.009	0.008	0.020	0.018	0.021	0.015	0.008	0.010	0.009

Compositions expressed as oxides quoted in wt.%

TABLE 5. COMPOSITION OF CORDIERITE, NORTHERN TALTSON MAGMATIC ZONE

Sample	*96B*	*40A*	*127A*	*30A*
FeO	6.56	7.15	7.10	7.49
MgO	9.73	9.21	10.14	9.71
SiO2	48.07	47.55	47.60	48.93
CaO	0.00	0.01	0.15	0.06
MnO	0.08	0.14	0.01	0.00
Al2O3	32.92	32.32	31.82	32.71
TOTAL	97.62	96.81	96.91	98.95
Fe/(Fe+Mg)	0.274	0.303	0.282	0.302

Compositions expressed as oxides quoted in wt.%

Monocyclic granulite-grade samples have general characteristics (Tracy 1982) that have been particularly well documented using whole-grain compositional maps (Tracy 1982, Pattison & Bégin 1994, Bégin & Pattison 1994). Garnet, cordierite, and orthopyroxene exhibit almost homogeneous values of Fe/(Fe + Mg), except within several hundred micrometers of adjacent ferromagnesian minerals, where steep Fe/(Fe + Mg) gradients (increasing in garnet, decreasing in orthopyroxene and cordierite) are produced by retrograde Fe–Mg exchange. The grossular component of the garnet shows minor variation regardless of adjacent minerals, and the Al content of the orthopyroxene is concentrically zoned to lower values in the rim, independent of adjacent minerals. Preservation of Al gradients in orthopyroxene that exhibit a uniform Fe/(Fe + Mg) has been interpreted to indicate that Al contents were frozen in at a temperature that still allowed diffusive homogenization of Fe/(Fe + Mg) (Fitzsimons & Harley 1994, Pattison & Bégin 1994). In order to retrieve equilibration temperatures approaching peak conditions, these authors used equilibria involving the Al content of orthopyroxene after adjusting Fe/(Fe + Mg) for the effects of retrograde Fe–Mg exchange. Computed conditions of equilibration, and related readjustment of mineral compositions, were based on the experimental data of Harley (1984).

Aranovich & Berman (1996, 1997) have advocated use of a more robust Al-in-Opx thermometer:

$$\text{Alm} = 3\text{ Fs} + \text{Al}_2\text{O}_3 \text{ (in orthopyroxene)} \qquad (7)$$

which they calibrated using reversed Al contents of FAS orthopyroxene in equilibrium with garnet and thermodynamic analysis of equilibria involving orthopyroxene, garnet, cordierite, ilmenite, and olivine (Berman & Aranovich 1996). They showed that this calibration yields reasonable agreement with Harley's experimental data on Al contents of orthopyroxene (calculated temperatures for run-product compositions generally within ±80°C of experimental temperatures using equilibrium 7), whereas computed Fe–Mg exchange temperatures based on the equilibrium

$$\text{Alm} + 3\text{ En} = 3\text{ Fs} + \text{Prp} \qquad (8)$$

were found to be in much poorer agreement with Harley's data. These comparisons suggest that Harley's unreversed Al contents are probably close to equilibrium values, whereas Fe/(Fe + Mg) values are in error, either because of Fe loss to Fe-capsules or nucleation of metastable Fe-rich garnet (Aranovich & Berman 1997). If this interpretation is correct, it implies that errors will also be inherent in adjustment of mineral compositions from Fe–Mg and Al-in-Opx temperature differences based on Harley's data.

Because of remaining uncertainties in the calibration of equilibrium (7), Aranovich & Berman (1997) cautioned against adjustment of mineral compositions in cases where the difference in Fe–Mg and Al-in-Opx temperatures are less than combined uncertainties, estimated to be ± 75°C. In the present study, we have used equation (7) for temperature estimates based on a recalibration (Berman & Aranovich, in prep.) that includes the same dataset described by Berman & Aranovich (1996), along with experimental data involving biotite and spinel. This recalibration leads to similarly good agreement with Harley's experimentally determined Al contents, but somewhat poorer agree-

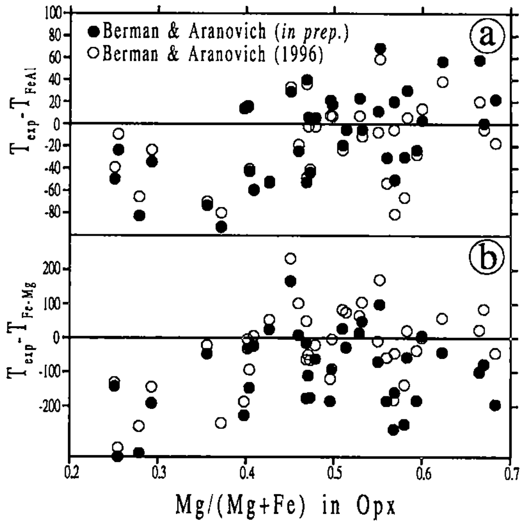

FIG. 7. Comparison of predicted and measured temperatures for Grt–Opx pairs produced experimentally by Harley (1984). Predictions use thermodynamic data of Berman & Aranovich (1996; open circles) and Berman & Aranovich (in prep.; filled circles). Note similarity between the two calibrations, and much closer correspondence with experiments of Al-in-Opx *versus* Fe–Mg exchange temperatures.

ment with his measured Fe/(Fe + Mg) values compared to the earlier calibration (Fig. 7). Most importantly, it removes some of the uncertainty in applications of equilibrium (7), and results in smaller differences between Fe–Mg and Al-in-Opx temperatures in natural samples (Berman & Aranovich, in prep.). Although differences for many samples are within combined calibration-imposed uncertainties (<50°C), larger differences for some samples suggest that adjustment of mineral compositions for the effects of retrograde Fe–Mg exchange is appropriate. In order to maintain intersample consistency, we therefore iteratively adjusted Fe/(Fe + Mg) of the orthopyroxene so as to yield identical temperatures with equilibrium (7) and (8) for each sample. Note that only subtle differences result if the Fe/(Fe + Mg) of garnet is adjusted rather than that of orthopyroxene.

For some samples, particularly those lacking orthopyroxene, temperature estimates have been obtained from the following Fe–Mg exchange equilibria:

$$2\ \mathrm{Alm} + 3\ \mathrm{Crd} = 3\ \mathrm{Skn} + 2\ \mathrm{Prp} \quad (9)$$

$$\mathrm{Alm} + \mathrm{Phl} = \mathrm{Ann} + \mathrm{Prp} \quad (10)$$

Owing to the evidence for retrograde Fe–Mg exchange discussed above and observed in zoning profiles presented below, Grt–Crd and Grt–Bt exchange temperatures should be regarded as minimum values.

Pressures were computed for Grt–Opx–Pl–Qtz and Grt–Crd–Sil–Qtz assemblages using the equilibria:

$$\mathrm{Alm} + \mathrm{Grs} + \mathrm{Qtz} = \mathrm{An} + \mathrm{Fs} \quad (11)$$

$$\mathrm{Grs} + 2\ \mathrm{Sil} + \mathrm{Qtz} = 3\ \mathrm{An} \quad (12)$$

$$\mathrm{Alm} + \mathrm{Sil} + \mathrm{Qtz} = \mathrm{Skn} \quad (13)$$

We assume that the grossular contents of garnet and the composition of plagioclase were quenched at the same time as the Al contents of the orthopyroxene, and therefore that pressures recorded with equilibrium (11) correspond to corrected Al-in-Opx temperatures. This assumption is supported by the similarity of available diffusion-coefficients for Ca in garnet and plagioclase (Brady 1975), both of which are significantly greater than Fe–Mg diffusivities in garnet (Chakraborty & Ganguly 1992). For samples without orthopyroxene, we assume that equilibrium (12) was quenched at a higher temperature than recorded by Grt–Crd exchange temperatures, and thus that pressures computed at the temperature recorded by equilibrium (9) or (10) are minimum values. Pressures resulting from the intersection of equilibria (9) and (13) are considered to be approximately correct, since retrograde Fe–Mg exchange shifts equilibrium (9) to lower temperature and equilibrium (13) to higher pressure.

Because of the evidence for closure of the above equilibria at different temperatures, we have not averaged the results for the entire assemblage using the INVQ technique (Gordon 1992). Instead, all calculations were performed with the TWQ software (Berman 1991) using internally consistent data for mineral end-members and solid solutions (TWQ version 2.02; Berman & Aranovich, in prep.). No attempt was made to retrieve quantitative P–T conditions from equilibria involving spinel (*e.g.*, Nichols *et al.* 1992), because concentrations of Zn and Fe^{3+} were not precisely determined in the microprobe analyses.

Results

Zoning profiles of orthopyroxene and garnet in samples of paragneiss and granite differ in several important respects from the general features of monocyclic granulites discussed above. Although rare orthopyroxene and garnet show flat core-to-rim Fe/(Fe + Mg) profiles, Fe/(Fe + Mg) varies in most larger grains, decreasing in orthopyroxene and increasing in garnet from core to rim, with irregularities that are spatially related to internal fractures (Fig. 8a). In orthopyroxene, this variation in Fe/(Fe + Mg) is mimicked by that in Al (Fig. 8a). These core-to-rim variations are apparent even in grains that are separated from each other (or from ilmenite) by quartz or feldspar or both (Fig. 8b). In general, the cores of larger grains of isolated orthopyroxene and garnet have higher and

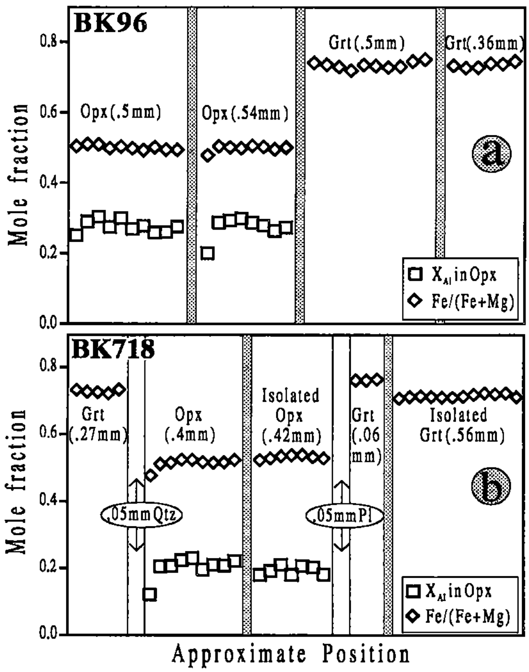

FIG. 8. Zoning profiles of orthopyroxene and garnet in samples (a) 96B and (b) 718B, determined by electron-microprobe analysis. The diameter of the grains is given in parentheses. Vertical lines indicate adjacent grains of orthopyroxene and garnet separated by quartz or plagioclase of specified size (grey: > 1 cm).

lower Fe/(Fe + Mg), respectively, than that of smaller grains. The most pronounced gradients in Fe/(Fe +Mg), and the most Fe-rich garnet and Fe-poor orthopyroxene, occur on either side of Opx–Grt interfaces, but even for non-touching grains, steeper gradients and more Fe-rich garnet and Fe-poor orthopyroxene occur in the rims of grains that are closer to another ferromagnesian mineral.

As temperatures attending granulite-facies metamorphism are too high to preserve growth-related zonation (Tracy 1982), the observed compositional gradients are interpreted to result from diffusional re-equilibration. The fact that gradients are observed in orthopyroxene and garnet that are surrounded by quartz or feldspar suggests that the re-equilibration must have taken place in the presence of an intergranular fluid medium, likely a silicate melt. Zoning profiles in orthopyroxene in monocyclic granulites have been interpreted to form during rapid cooling upon extraction of melt after a period of high-temperature re-equilibration during which Al gradients were established and Fe/(Fe + Mg) became homogenized (Bégin & Pattison 1994). The contrasting zoning patterns in the TMZ may indicate a period of cooling in the presence of a melt that established Fe/(Fe + Mg) and Al gradients, followed by cooling that was rapid enough to quench both gradients.

Two observations, however, suggest that the observed zoning profiles result from re-equilibration induced by a later episode of heating. The first is the resetting of Fe/(Fe + Mg) and Al adjacent to fractures in individual grains. The second is the not-uncommon finding, in the immediate rim of some grains of orthopyroxene, of reversals in the core-to-rim decrease in Fe/(Fe + Mg) and Al (Figs. 8a, b). In samples with relatively less garnet than orthopyroxene, core-to-rim reversals in Fe/(Fe + Mg) also are observed in some grains of garnet (*e.g.*, 0.56 mm grain of garnet, Fig. 8b). We interpret these reversals as resulting from a later, short-lived episode of reheating related to emplacement of the Konth granite. In several granitic samples, some orthopyroxene rims adjacent to garnet show a sharp decrease, whereas others show a sharp increase in Al. These differences may reflect local differences in bulk composition during the late episode of reheating. In order to retrieve near-peak temperatures, we used cores of proximal grains of garnet and orthopyroxene that are separated from one another by quartz or feldspar or both for our thermobarometric calculations. As the above observations indicate that compositions of even the largest grains of orthopyroxene and garnet have been reset to some extent, derived P–T estimates are likely minimum values.

TABLE 6. P–T RESULTS FOR Opx-BEARING SAMPLES FROM THE NORTHERN TALTSON MAGMATIC ZONE

Sample	T_7-P_{11}	T_7*-P_{11}	ΔOpx	T_{10}
258A	965-7.6	1025-7.4	.03	-
353A	880-6.8	970-6.5	.09	765
317A	930-7.4	1005-7.1	.06	905
2063	980-6.5	1045-6.2	.07	690
310A	915-6.2	945-6.15	.03	-
718A	905-6.2	920-6.0	.015	710
59B	650-7.6	870-7.6	-	885
145B	890-7.8	970-7.7	.07	740
187C	940-7.9	985-7.8	.03	860
223B	910-6.4	920-6.4	.005	690
505B	875-6.6	885-6.5	.005	710
106B	925-6.7	945-6.6	.01	-
96B	970-7.6	1020-7.4	.04	750
40A	865-5.2	875-5.2	.07	910
59A	825-5.7	860-5.65	.03	740

T_7, T_{10} and P_{11} are values computed from equilibria 7, 10 and 11, respectively.
T_7* = t_7 after adjustment of Fe/(Fe + Mg) value of Opx by Δopx (see text).

Plagioclase in samples of paragneiss and in most samples of granite shows only minor variations in composition, generally less than ±3 mol.% An, with subtle reverse zoning in larger grains of some samples and normal zoning in other samples. In several samples of granite, large phenocrysts of plagioclase are

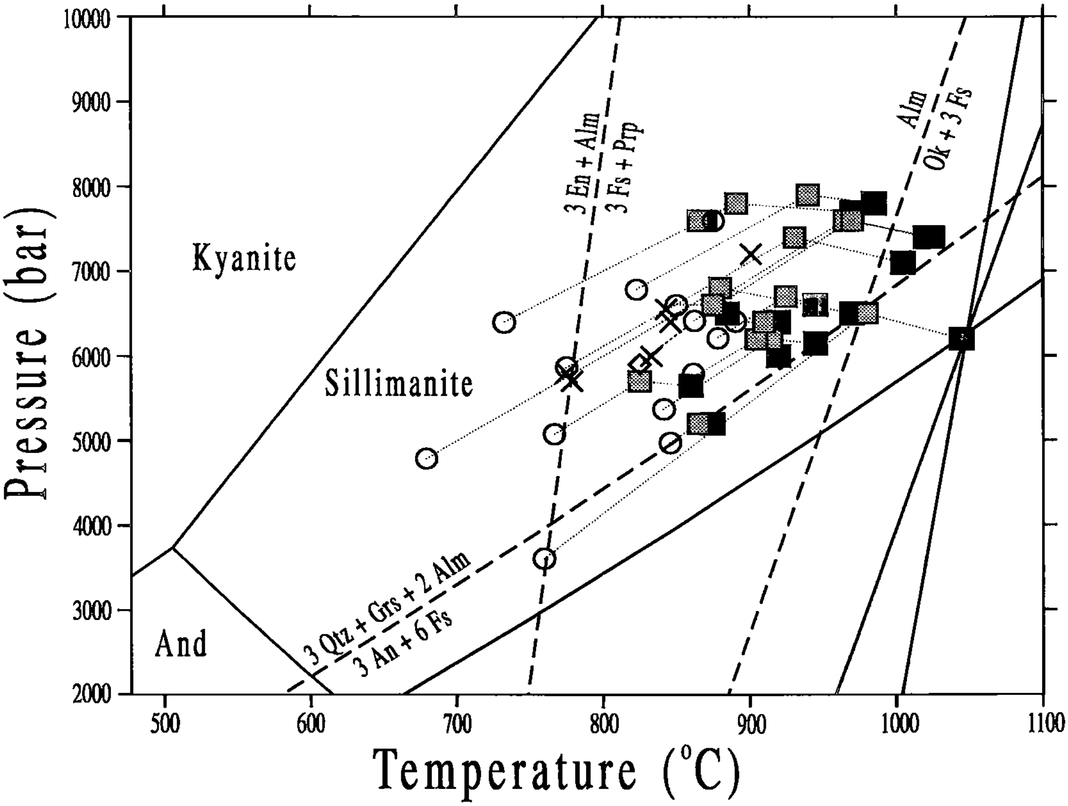

FIG. 9. Thermobarometry results for the Taltson Magmatic Zone, taken from Tables 6 and 7. Shaded and filled boxes give P–T values using equilibria (7) and (11) with nominal and adjusted (see text) Fe/(Fe + Mg) in orthopyroxene, respectively. Circles are P–T values based on equilibria (8) and (11) and unadjusted compositions of minerals. Crosses are P–T values based on equilibria (9), (12), and (13) and unadjusted compositions of minerals. Ok: Al_2O_3 in orthopyroxene.

normally zoned (ΔCa = 0.07), with rims having the same composition as small, polygonal grains that formed at their grain boundaries. In thermobarometric calculations, we used average compositions of plagioclase, or rim compositions for granitic samples with significant zoning in the plagioclase grains.

Calculated P–T results for orthopyroxene-bearing rocks are listed in Table 6. With the exception of one sample (59A), uncorrected Al-in-Opx temperatures are higher than Fe–Mg exchange temperatures by between 20 and 200°C (Fig. 9). Increasing the Fe/(Fe + Mg) of orthopyroxene yields a large increase in the Fe–Mg temperature (equilibrium 8), but a relatively small increase in the Al-in-Opx temperature due to the large change in enthalpy of equilibrium (7). Corrected pressures decrease slightly. Whereas the uncorrected Fe–Mg temperatures range from 680 to 890°C, uncorrected Al-in-Opx temperatures form a much tighter group, between 865 and 980°C. Not included in this range are two samples with the lowest Al-in-Opx temperatures (650, 825°C) that show the greatest development of a late rim of biotite on orthopyroxene or fractured orthopyroxene and grains of garnet with prominent alteration of feldspar. Corrected temperatures are between 860 and 1045°C for all samples, with 11 of 15 samples showing temperatures above 920°C. Pressures vary between 6.0 and 7.8 kbar, with no obvious geographic pattern (Fig. 10). Samples of paragneiss do not show significantly different values than samples of granite.

Calculated Grt–Crd temperatures are listed in Table 7. For one sample in which both orthopyroxene and cordierite were analyzed, the Grt–Crd thermometer yields slightly lower temperatures than the Grt–Opx exchange temperature, suggesting that retrograde Fe–Mg exchange has affected the Grt–Crd thermometer in the same manner as the Grt–Opx thermometer. As discussed above, because Grt–Crd-derived temperatures cannot be corrected for this effect, Grt–Crd values represent minimum temperatures only. Nevertheless, it is interesting to note that as with Grt–Opx exchange temperatures, most values are above 800°C, and a few

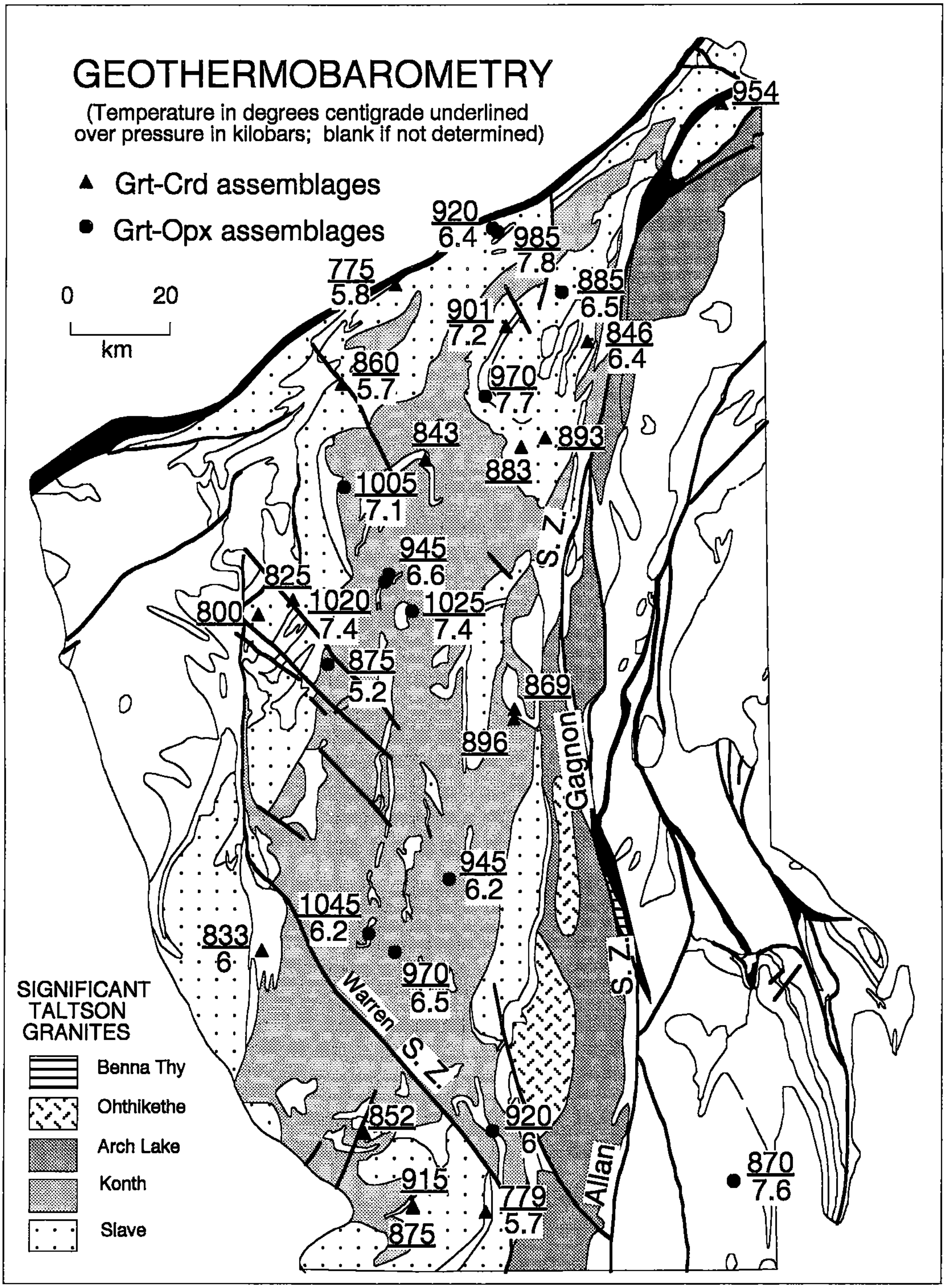

FIG. 10. Regional distribution of thermobarometry results.

TABLE 7. P–T RESULTS FOR Grt–Crd SAMPLES FROM THE NORTHERN TALTSON MAGMATIC ZONE

Sample	T_9	P_{13}	P_{12}
96B	800	< 7.9	-
127A	775	5.8	5.1
30A	825	6.6	6.5
780A	833.4	6.0	-
484A	617.4	< 3.3	-
797A	852.1	< 7.8	-
879A	875	< 6.9	-
880A	915	< 7.3	-
493A	778.7	5.7	-
736A	895.6	< 7.3	-
760A	869	< 6.3	-
387C	892.7	< 8.2	-
403A	883.2	< 7.2	-
105A	901.2	7.15	-
319C	845.8	6.4	-

T_9, P_{13}, P_{12} are values computed from equilibria 9, 13 and 12 respectively.

are as high as 900°C (Fig. 9). Grt–Crd exchange temperatures computed with the compositions reported by Nielsen *et al.* (1981) for the southern TMZ show a similar range of values, shifted to lower temperatures by about 50°C. Given the sensitivity of thermobarometric results to details of textural relationships, we do not consider this difference to be significant.

Computed Grt–Bt exchange temperatures (Table 6) are, for the most part, considerably lower than Grt–Opx or Grt–Crd temperatures, consistent with textural indications of late crystallization of biotite. In samples with sparse, coarse biotite separated from orthopyroxene and garnet by quartz or feldspar, Grt–Bt exchange temperatures are comparable to those given by the other exchange thermometers.

The thermometry results presented above are comparable to regional determinations from the southern TMZ, which range between 800–850°C (Grover *et al.* 1997) and 700–750°C (Nielsen *et al.* 1981). Because they are based on Crd–Grt compositions that very likely have been open to late Fe–Mg exchange (see above), we infer that maximum termperatures in the southern TMZ were not significantly different from those determined in this study. This conclusion is supported by 950–1000°C temperatures obtained for southern TMZ samples by oxygen isotope systematics (Farquhar *et al.* 1994) and TWQ thermometry (Chacko *et al.* 1994). Given the patchy occurrence of orthopyroxene found in the northern TMZ paragneiss, its absence in the samples studied from the southern TMZ by Grover *et al.* (1997) is probably not significant, being a function of the less detailed sampling density or of slightly more aluminous bulk compositions compared to the northern TMZ (or both).

Temperatures in the TMZ do, however, seem to have been somewhat higher than those attending metamorphism in the adjacent Thelon tectonic zone (TTZ) to the north. This conclusion is based on the general lack of reported occurrences of the assemblage Spl + Qtz in the TTZ (Thompson *et al.* 1986, James 1989), as well as results from thermometry. Al-in-Opx temperatures calculated as described above, using the few available compositions of minerals in the TTZ (James 1989, Haggert 1987) yield maximum temperatures of 850°C at ~7.5 kbar, with most samples recording temperatures less than 800°C.

Discussion

The western margin of Rae Province comprises a Paleoproterozoic, mixed gneiss terrane with local isotopic inheritance from an Archean precursor, indicated by the presence of ~3.0 Ga zircon north of 60°N (Bostock *et al.* 1991), and minor tectonic slices of Archean (3.04–3.2 Ga) gneiss in the basement complex in northeastern Alberta (McDonough *et al.* 1995). Widespread granitic magmatism occurring between 2.45 and 2.27 Ga (Burwash *et al.* 1985, Bostock *et al.* 1987, Bostock & Loveridge 1988, Bostock *et al.* 1991) has been interpreted to indicate an Early Proterozoic convergent tectonic setting (Hoffman 1988). Subsequent rifting, suggested by the emplacement of mafic to ultramafic rocks, produced the Rutledge River basin (Bostock & van Breemen 1994). Similarities of ϵ_{Nd} and zircon geochronology between the Buffalo Head terrane and western Rae Province (Thériault & Ross 1991, Ross *et al.* 1991, Thériault 1994) suggest that the former may represent the rifted portion of the western Rae Province that produced this basin. The age of metamorphic monazite constrains basin closure to be prior to 2.09 Ga (Bostock & van Breemen 1994).

The succeeding Taltson plutonism has been considered on the basis of geochemical and ϵ_{Nd} data (Thériault 1992) to comprise pre- and postcollisional components. The Deskenatlata granite (1.99 Ga) has uniform ϵ_{Nd} values (–2.7 to –3.6) taken to indicate mixing and homogenization of batches of mantle-derived melt with older continental crust (Thériault 1992) in a precollisional, continental magmatic arc. The peraluminous Slave (1.96 Ga) granite has ϵ_{Nd} values (–4.4 to –8.6) in the same range as gneisses of the Buffalo Head terrane and western Rae Province, consistent with derivation of the Slave granite through melting of a significant proportion of these crustal components in a collisional setting. The more restricted range of ϵ_{Nd} (–4.7 to –5.5) of the peraluminous Konth (1.94–1.93 Ga) granite is within the range of paragneiss xenoliths (–4.1 to –6.0), suggesting that the sedimentary rocks of the Rutledge River Basin were the primary source-rocks of the Konth granite.

The distribution of metamorphic parageneses (Fig. 4) lends support to the geochemically derived model for the evolution of the TMZ, and allows some refinement of it. The general lack of granulite-facies assemblages (Opx, Grt–Crd–Kfs; Figs. 4a, c) and the predominance of biotite in the mixed gneisses of the northern fault-wedges of the Rae Province and the Deskenatlata suite indicate that 2.45–2.27 Ga and 1.99 Ga magmatism were characterized by lower temperatures and conditions of higher H_2O activity. Widespread occurrence of orthopyroxene and of the assemblage Grt–Crd–Kfs in the subsequent intrusive bodies and paragneiss xenoliths within them attests to higher temperatures and conditions of lower H_2O activity between 1.96 and 1.93 Ga. The concentration of occurrences of the assemblage Spl + Qtz within the central portion of the Konth granite suggests that the highest temperatures were attained during the latest stage of TMZ plutonism. This progression from low- to high-temperature plutonism and associated metamorphism between 1.99 and 1.93 Ga are consistent with early arc plutonism followed by plutonism in increasingly thickened crust within a collisional orogen. Rising isotherms within the thickening orogen would allow the locus of melting to rise with time from basement levels (Buffalo Head and Rae Province gneisses) to the level of supracrustal rocks (Rutledge River Basin), as suggested by the geochemical data (Thériault 1992).

Geothermobarometry results indicate a roughly constant level of exposure of 6.9 ± 0.9 kbar, corresponding to approximately 21 km of removal by erosion for the northern TMZ. Al-in-Opx geothermometry recorded by granites and paragneiss xenoliths generally shows higher temperatures within the Konth granite compared to the Slave granite, although Slave temperatures may be reset during the subsequent Konth intrusion. Within the Konth granite, temperatures do not show exactly the same spatial pattern as the distribution of the assemblage Spl + Qtz. The most likely reason for this distinction is variable extent of re-equilibration of the assemblage Grt–Opx during cooling and late-stage deformation (see below). Of particular importance, however, is the finding that recorded temperatures, although likely minimum values, are consistently in the range 920–1045°C.

Near-peak TMZ temperatures are in excellent agreement with experimental evidence that leucogranites akin to the TMZ granitic rocks can be produced by dehydration melting of a pelite bulk-composition at temperatures above 825–850°C. Experimental investigations of the melting behavior of pelitic bulk-compositions (Vielzeuf & Holloway 1988, Le Breton & Thompson 1988, Patiño Douce & Johnston 1991, Patiño Douce & Beard 1995) demonstrate that large volumes of granitic melt (up to ~60% of source rock) can be produced through dehydration melting of a pelitic source-rock, with the largest volumes of melt derived from plagioclase-rich pelites. Results of Patiño Douce & Johnston (1991) show that compositions of experimentally produced melts (~70 wt % SiO_2, 2–5 wt % normative corundum, MgO + FeO + TiO_2 < 3 wt %) are like those of leucogranites produced in continental collision environments (*e.g.*, Himalayan-type), and very similar to compositions of the Slave and Konth granites (Thériault 1992). Experiments at 7 kbar indicate initiation of biotite-dehydration melting above 825–875°C (Patiño Douce & Johnston 1991, Patiño Douce & Beard 1995) *via* the reaction

$$\text{Bt} + \text{Als} + \text{Qtz} \pm \text{Pl, Ilm} = \text{Granitic melt} + \text{Grt} \pm \text{Rt},$$

with volume of melt and normative corundum increasing, and activity of H_2O decreasing with increasing temperature. At 7 kbar, the pressure recorded by TMZ samples, the proportion of modal biotite decreases with increasing temperature, until its disappearance above ~950°C (Patiño Douce & Johnston 1991, Patiño Douce & Beard 1995). The correspondence of these temperatures with near-peak temperatures in the TMZ results is striking, and provides an explanation for the general lack of primary biotite in the Slave and Konth granites. By way of contrast, those paragneiss samples that contain abundant early biotite likely represent protoliths rather than restite material. At 925–950°C, maximum productivity of melt in a plagioclase-rich bulk composition (~50 vol.%) was found at an intermediate pressure of 7 kbar (Patiño Douce & Beard 1995). Above 975°C at 7 kbar, melting proceeds *via* the reaction (Patiño Douce & Johnston 1991):

$$\text{Grt} + \text{Als} = \text{Melt} + \text{Spl} + \text{Qtz}.$$

These P–T conditions again correspond closely to those obtained on TMZ samples, particularly in the central portion of the Konth granite (Fig. 10), which shows the greatest abundance of rocks with the assemblage Spl + Qtz (Fig. 4d).

An interesting aspect of the regional thermometry results is their comparison with temperatures predicted by conductive thermal models of tectonically thickened crust. Such models show that the maximum temperature reached during thickening of continental crust is between ~850°C (England & Thompson 1986, Thompson & Connolly 1995) and 910°C (Patiño Douce *et al.* 1990), the higher value associated with a thinned lithosphere model. These models require that a mechanism be established for increasing the temperature in the TMZ above those obtained in these numerical simulations. An additional consideration is the higher temperature that apparently attended magmatism in the TMZ compared to its northern extension in the Thelon tectonic zone.

The most commonly invoked mechanism to augment overall temperature, and one usually inferred from counterclockwise P–T–t paths with late isobaric cooling, is the addition of heat from basaltic magma underplating the crust (Wells 1980, Harley 1989, Bohlen 1991, Waters 1991). However, Nd isotopic data (Thériault 1992) do not show a mantle component in the Slave and Konth granites, nor do field relationships indicate a significant mafic component in the 1.96–1.93 Ga plutonism. In addition, although the post-peak P–T path is dominated by successive cooling through model reactions 5, 2, and 1 prior to late crystallization of andalusite, the occurrence in some paragneiss samples of garnet inclusions in orthopyroxene (see above), as well as the report of kyanite from Pilot Lake granitic gneiss (Burwash & Cape 1981), may be indicative of an early clockwise P–T–t path prior to the thermal peak. As an alternative, these features may be relics of the ~2.09 Ga metamorphism inferred from geochronological data (Bostock & van Breemen 1994).

An effective mechanism in achieving markedly higher temperatures in thermal models of collisional orogens is increased production of radiogenic heat due to the greater abundance of radiogenic isotopes in the Paleoproterozoic compared to present-day crustal rocks (Chacko 1997). This mechanism cannot, however, account for the lower temperatures inferred for the TTZ relative to the TMZ. The same criticism applies to the higher temperatures predicted in thermal models that involve heat convection from the lower crust to mid-crust levels. One contributing factor to the production of higher temperatures at ~1.94 Ga is preheating by the earlier Deskenatlata (~1.99 Ga) and Slave (~1.96 Ga) intrusions, which could have produced a regime of elevated temperature at the top of the underthrust Buffalo Head terrane for more than 30 Ma (Ashwal *et al.* 1992). Another possibility unique to the TMZ is increased flux of mantle-derived heat as a consequence of subduction of an oceanic ridge following subduction of oceanic crust to produce the Deskenatlata suite (G.M. Ross, pers. commun.), or delamination of lithosphere. The latter possibility is considered unlikely because of the lack of evidence in the TMZ for postcollisional extension predicted in delamination models (*e.g.*, Platt & England 1994).

Polymetamorphism in the Taltson Magmatic Zone

On the basis of mineral chemistry, textural evidence, and Rb–Sr geochronology, previous work in the TMZ in northeastern Alberta (Nielsen *et al.* 1981) suggests a polymetamorphic history, with Archean (> 2.47 Ga) high-P – high-T granulite-facies metamorphism (M_1), followed by ~1.94 medium-P – medium-T granulite- ($M_{2.1}$) and later amphibolite- ($M_{2.2}$) and greenschist-facies ($M_{2.3}$) metamorphism. P–T conditions of 900 ± 100°C – 7.5 ± 2 kbar were estimated for M_1 from petrogenetic-grid constraints on the occurrence of the assemblage Cpx–Opx–Spl–Sil–Crn, whereas thermobarometry yielded 740 ± 30°C and 5.0 ± 0.7 kbar for $M_{2.1}$ (Nielsen *et al.* 1981). Similar metamorphic conditions were obtained from the Western Granulite domain of Saskatchewan (P.A. Nielsen, pers. commun. reported in Lewry *et al.* 1985), although Lewry *et al.* (1985) considered the $M_{2.1}$ event in northeastern Alberta to be Archean in age. The current geochronological database indicates an extensive Paleoproterozoic tectonothermal history for the gneisses of the Rae Province and Taltson basement complex, with only local suggestion of Archean protoliths. Similarly, Crocker *et al.* (1985) found some evidence for metamorphism as old as 2.9 Ga in anorthosite in southwestern Saskatchewan, but they interpreted major tectonothermal events at ~2.3–2.2 Ga, ~2.1–1.9 Ga, and ~1.8 Ga. The evidence for ~950°C metamorphism producing the assemblage Spl–Qtz between 1.96 and 1.93 Ga demonstrates that Taltson plutonism was responsible for the highest-grade mineral assemblages, with somewhat lower-grade conditions characterizing granitic gneisses of the Rae Province that form the extension of the Taltson basement complex in northern Alberta. Similarly, the Taltson basement complex in northeastern Alberta is characterized by somewhat lower-grade assemblages than the TMZ paragneiss to the west (Grover *et al.* 1997). These observations suggest that the M_1 event of Nielsen *et al.* (1981) is an upper-amphibolite facies, Paleoproterozoic, ~2.4–2.1 Ga event, although Burwash *et al.* (1985) did report evidence for 2.44 Ga granulite-facies metamorphism in mafic xenoliths within the Slave granite from Mountain Rapids, Alberta. The lower-P – lower-T conditions ascribed by Nielsen *et al.* (1981) to their $M_{2.1}$ event undoubtedly result from their analysis of partially re-equilibrated Grt–Crd assemblages, as documented in this study.

High-grade mineral assemblages, comparable to those within the TMZ except for their more substantial greenschist-facies retrogression, occur in the paragneiss-bearing fault blocks of the southwestern Rae Province that pinch out north of Lady Grey Lake (Figs. 2, 4). That some fractions of monazite within the paragneiss in this region yield U–Pb ages that are only slightly younger than the Konth batholith suggests high-temperature resetting of this region (Bostock & van Breemen, in prep.). The northern Rae Province fault blocks bear similar plutonic lithologies, but lack the metamorphic orthopyroxene that characterizes the high-temperature TMZ event. Restoration of these two fault-bounded blocks of Rae Province regions toward their original positions along the major sinistral Tazin and Allan shear zones (Figs. 2, 3) is consistent with the view that the two blocks represent the interior, higher-grade (southern block) and exterior, lower-grade (northern block) portions of a metamorphic belt at the time of the Konth intrusion. Such an interpretation also is consistent with eastward overlap of Rutledge River sedimentary rocks being limited to the southern fault-blocks.

Earlier metamorphism within the TMZ is constrained between 2.08 and 2.05 Ga on the basis of

U–Pb monazite ages in paragneiss from Rutledge Lake (Bostock & van Breemen 1994). Zircon of similar age from paragneiss samples near Tsu Lake and Thubun Lakes (Fig. 1) suggest that this metamorphism was widespread. Of particular interest is the fact that all monazite samples analyzed from paragneiss within the Konth granite yield 1.93 Ga Konth ages, and all but two samples from paragneiss in the 1.96 Ga Slave granite also yield Konth or slightly younger ages (Bostock & van Breemen, in prep.). This widespread isotopic resetting during the Konth magmatic phase probably produced the evidence for chemical re-equilibration observed in the zoning profiles discussed above, and could also account for the late crystallization of sillimanite around andalusite porphyroblasts observed in some samples.

Evidence for the $M_{2.3}$ greenschist-facies metamorphism described by Nielsen *et al.* (1981) is widespread but sporadic, being most evident in shear zones that show late movement and brittle behavior. K–Ar and $^{40}Ar/^{39}Ar$ data (Plint & McDonough 1995) indicate protracted cooling from 725°C at ~1.93 Ga (monazite), through ~525°C at 1.9 Ga ($^{40}Ar/^{39}Ar$ in hornblende), to ~350°C at 1.8 Ga (K–Ar, muscovite). The Ar geochronometry has been interpreted to reflect cooling during isostatic uplift, with shear-zone deformation at amphibolite to greenschist grade between 1.9 and 1.86 Ga, followed by greenschist-facies deformation (Plint & McDonough 1995). Grt–Crd–Kfs assemblages within mylonite zones of the southern TMZ (Grover *et al.* 1997), however, indicate initial formation of shear zones under lower granulite-facies conditions. Comparison of the above isotopic data with monazite ages as young as 1.88 Ga from samples proximal to shear zones on the northern and western flanks of the northern TMZ (Bostock & van Breemen, in prep.) indicates that extent of monazite closure to isotopic re-equilibration was strongly affected by recrystallization during late deformation concentrated in some shear zones.

Acknowledgements

We gratefully acknowledge the assistance of John Stirling with electron-microprobe operation, Gordon Pringle with microprobe-data reduction, Dave Walker with SEM analyses, and Katherine Venance with drafting and electron-microprobe analysis. We also thank R. Thériault, P. Nielsen, A. Patiño-Douce, and M. Easton for the constructive reviews provided.

References

Aranovich, L.Y. & Berman, R.G. (1996): Optimized standard state and mixing properties of minerals. II. Comparisons, predictions, and applications. *Contrib. Mineral. Petrol.* **126**, 25-37.

________ & ________ (1997): A new garnet-orthopyroxene thermometer based on reversed Al_2O_3 solubility in $FeO–Al_2O_3–SiO_2$ orthopyroxene. *Am. Mineral.* **82**, 345-353.

Ashwal, L.D., Morgan, P. & Hoisch, T.D. (1992): Tectonics and heat sources for granulite metamorphism of supracrustal-bearing terranes. *Precambrian Res.* **55**, 525-538.

Aspler, L.B. & Donaldson, J.A. (1986): The Nonacho basin (Early Proterozoic), Northwest Territories, Canada: sedimentation and deformation in a strike-slip setting. *In* Strike-Slip Deformation, Basin Formation, and Sedimentation (K.T. Biddle & N. Christie-Bick, eds.). *Soc. Econ. Paleontol. Mineral., Spec. Publ.* **37**, 193-209.

Audibert, N., Hensen, B.J. & Bertrand, P. (1995): Experimental study of phase relations involving osumilite in the system $K_2O–FeO–MgO–Al_2O_3–SiO_2–H_2O$ at high pressure and temperature. *J. Metamorphic Geol.* **13**, 331-344.

Bégin, N.J. & Pattison, D.R.M. (1994): Metamorphic evolution of granulites in the Minto block, northen Quebec: extraction of peak P–T conditions taking account of late Fe–Mg exchange. *J. Metamorphic Geol.* **12**, 411-428.

Berman, R.G. (1991): Thermbarometry using multiequilibrium calculations: a new technique with petrological applications. *Can. Mineral.* **29**, 833-856.

________ & Aranovich, L.Y. (1996): Optimized standard state and mixing properties of minerals. I. Model calibration for olivine, orthopyroxene, cordierite, garnet, and ilmenite in the system $FeO–MgO–CaO–Al_2O_3–SiO_2–TiO_2$. *Contrib. Mineral. Petrol.* **126**, 1-24.

Bohlen, S.R. (1991): On the formation of granulites. *J. Metamorphic Geol.* **9**, 223-229.

Bostock, H.H. (1984): Preliminary geological reconnaissance of the Hill Island Lake and Taltson Lake areas, District of Mackenzie. *Geol. Surv. Can., Pap.* **84-1A**, 165-170.

________ (1992): Local geological investigations in Hill Island Lake area, District of Mackenzie, Northwest Territories. *Geol. Surv. Can., Pap.* **92-1C**, 217-223.

________ & Loveridge, W.D. (1988): Geochronology of the Taltson Magmatic Zone and its eastern Cratonic Margin, District of Mackenzie. *In* Radiometric Age and Isotopic Studies. *Geol. Surv. Can., Pap.* **88-2**, 59-65.

________ & van Breemen, O. (1994): Ages of detrital and metamorphic zircons from a pre-Taltson magmatic zone basin at the western margin of Churchill Province. *Can. J. Earth Sci.* **31**, 1353-1364.

________, ________ & Loveridge, W.D. (1987): Proterozoic geochronology in the Taltson Magmatic Zone, N.W.T. *In* Radiometric Age and Isotopic Studies. *Geol. Surv. Can., Pap.* **87-2**, 73-80.

________, ________ & ________ (1991): Further geochronology of plutonic rocks in northern Taltson Magmatic Zone, District of Mackenzie, N.W.T. *In* Radiometric Age and Isotopic Studies. *Geol. Surv. Can., Pap.* **91-4**, 67-78.

BRADY, J.B. (1975): Reference frames and diffusion coefficients. *Am. J. Sci.* **275**, 954-983.

BURWASH, R.A. & CAPE, D.F. (1981): Petrology of the Fort Smith – Great Slave Lake radiometric high near Pilot Lake, N.W.T. *Can. J. Earth Sci.* **18**, 842-851.

________, KRUPICKA, J., BASU, A.R. & WAGNER, P.A. (1985): Resetting of Nd and Sr whole-rock isochrons from polymetamorphic granulites, northeastern Alberta. *Can. J. Earth Sci.* **22**, 992-1000.

CARRINGTON, D.P. (1995): The relative stability of garnet – cordierite and orthopyroxene – sillimanite – quartz assemblages in metapelitic granulites: experimental data. *Eur. J. Mineral.* **7**, 949-960.

CHACKO, T. (1997): Ultra-high temperature metamorphism at Pelican Rapids, Taltson Magmatic zone, NE Alberta: possible implications for early Proterozoic orogens. *Geol. Assoc. Can. – Mineral. Assoc. Can., Program Abstr.* **22**, A24.

________ & CREASER, R.A. (1995): Hercynite-bearing granites and associated metasedimentary enclaves from the Taltson magmatic zone, Alberta, Canada: a natural example of high-temperature pelite melting. *In* The Origin of Granites and Related Rocks (M. Brown & P.M. Piccoli, eds.). *U.S. Geol. Surv., Circ.* **1129**, 161-162.

________, ________ & POON, D. (1994): Spinel + quartz granites and associated metasedimentary enclaves from the Taltson magmatic zone, Alberta, Canada: a view into the root zone of a high-temperature, S-type granitic batholith. *Mineral. Mag.* **58A**, 161-162.

CHAKRABORTY, S. & GANGULY, J. (1992): Cation diffusion in aluminosilicate garnets: experimental determination in spessartine-almandine diffusion couples, evaluation of effective binary diffusion coefficients, and applications. *Contrib. Mineral. Petrol.* **111**, 74-86.

CLARKE, G.L. & POWELL, R. (1991): Proterozoic granulite facies metamorphism in the southeastern Reynolds Range, central Australia – geological context, P–T path and overprinting relationships. *J. Metamorphic Geol.* **9**, 267-281.

CROCKER, C.H., COLLERSON, K.D., LEWRY, J.F. & BICKFORD, M.E. (1985): Sm–Nd, U–Pb, and Rb–Sr geochronology and lithostructural relationships in the southwestern Rae province: constraints on crustal assembly in the western Canadian shield. *Precambrian Res.* **61**, 27-50.

DAVIDSON, A., CARMICHAEL, D.M. & PATTISON, D.R.M. (1990): Field Guide to the Metamorphism and Geodynamics in the southwestern Grenville Province, Ontario. *Int. Geol. Correlation Program, Project* **235/304**, *Fieldtrip Guide* **1**.

DE CAPITANI, C. & BROWN, T.H. (1987): The computation of chemical equilibrium in complex systems containing non-ideal solutions. *Geochim. Cosmochim. Acta* **51**, 2639-2652.

ENGLAND, P.C. & THOMPSON, A.B. (1986): Some thermal and tectonic models for crustal melting in continental collision zones. *In* Collision Tectonics (M.P. Coward & A.C. Ries, eds.). *Geol. Soc. Am., Spec. Pap.* **19**, 83-94.

FARQUHAR, J., CHACKO, T. & ELLIS, D.J. (1994): High-temperature oxygen isotope thermometry in two contrasting terranes, the Taltson Magmatic Zone, Canada and the Napier Complex, Antarctica. *Mineral. Mag.* **58A**, 265-266.

FITZSIMONS, I.C.W. (1996): Metapelitic migmatites from Brattstrand Bluffs, East Antarctica – metamorphism, melting, and exhumation of the mid crust. *J. Petrol.* **37**, 395-414.

________ & HARLEY, S.L. (1994): Disequilibrium during retrograde cation exchange and recovery of peak metamorphic temperatures: a study of granulites from Antarctica. *J. Petrol.* **35**, 543-576.

GIBB, R.A. (1978): Slave–Churchill collision tectonics. *Nature* **271**, 50-52.

GODFREY, J.D. & LANGENBERG, C.W. (1978): Metamorphism in the Canadian Shield of NE Alberta. *In* Metamorphism in the Canadian Shield (J.A. Fraser & W.W. Heywood, eds.). *Geol. Surv. Can., Pap.* **78-10**, 129-138.

GORDON, T.M. (1992): Generalized thermobarometry: solution of the inverse geochemical problem using data from individual species. *Geochim. Cosmochim. Acta* **56**, 1793-1800.

GROVER, T.W., PATTISON, D.R.M., MCDONOUGH, M.R. & MCNICOL, V.J. (1997): Tectonometamorphic evolution of the southern Taltson magmatic zone and associated shear zones, northeastern Alberta. *Can Mineral* **35**,

HAGGERT, M.J. (1987): *Geothermobarometry of the Slave–Churchill Structural Provinces Boundary, Artillery Lake Map Area, District of Mackenzie*. M.Sc. thesis, Queen's Univ., Kingston, Ontario.

HANMER, S., BOWRING, S., VAN BREEMEN, O. & PARRISH, R. (1992): Great Slave Lake Shear Zone, NW Canada: mylonitic record of early Proterozoic continental convergence, collision and indentation. *J. Struct. Geol.* **14**, 757-773.

HARLEY, S.L. (1984): The solubility of alumina in orthopyroxene coexisting with garnet in FeO–MgO–Al_2O_3–SiO_2 and CaO–FeO–MgO–Al_2O_3-SiO_2. *J. Petrol.* **25**, 665-696.

________ (1989): The origins of granulites: a metamorphic perspective. *Geol. Mag.* **126**, 215-247.

HEAMAN, L.M. & PARRISH, R.R. (1991): U–Pb geochronology of accessory minerals. *In* Application of Radiogenic

Isotope Systems to Problems in Geology (L.M. Heaman & J.N. Ludden, eds.). *Mineral. Assoc. Can., Short Course Handbook* **19**, 59-102.

HENSEN, B.J. & GREEN, D.H. (1973): Experimental study of the stability of cordierite and garnet in pelitic compositions at high pressure and temperatures. III. Synthesis of experimental data and geological applications. *Contrib. Mineral. Petrol.* **38**, 151-166.

HOFFMAN, P.F. (1988): United Plates of America. *Annu. Rev. Earth Planet. Sci.* **16**, 543-603.

JAMES, D.T. (1989): *Geology of the Thelon Tectonic Zone in the Moraine Lake Area, District of Mackenzie, Northwest Territories: the Definition and Significance of Lithologic, Structural and Metamorphic Changes Across the Boundary between the Slave and Churchill Structural Provinces*. Ph.D. thesis, Queen's Univ., Kingston, Ontario.

KRETZ, R. (1983) Symbols for rock-forming minerals. *Am. Mineral.* **68**, 277-279.

LANDENBERGER, B. & COLLINS, W.J. (1996): Derivation of A-type granites from a dehydrated charnockitic lower crust: evidence from the Chaelundi Complex, eastern Australia. *J. Petrol.* **37**, 145-170.

LE BRETON, N. & THOMPSON, A.B. (1988): Fluid-absent (dehydration): melting of biotite in metapelites in the early stages of crustal anatexis. *Contrib. Mineral. Petrol.* **99**, 226-237.

LEWRY, J.F., SIBBALD, T.I.I. & SCHLEDEWITZ, D.C.P. (1985): Variation in character of Archean rocks in the western Churchill Province and its significance. *In* Evolution of Archean Supracrustal Sequences (L.D. Ayres, P.C. Thurston, K.D. Card & W. Weber, eds.). *Geol. Assoc. Can., Spec. Pap.* **28**, 239-261.

MCDONOUGH, M.R., MCNICOLL, V.J. & SCHETSELAAR, E.M. (1995): Age and kinematics of crustal shortening and escape in a two-sided oblique-slip collisional and magmatic orogen, Paleoproterozoic Taltson magmatic zone, northeastern Alberta. *In* Alberta Basement Transects Workshop **47** (G.M. Ross, ed.). University of British Columbia, Vancouver, British Columbia (264-308).

MULLIGAN, R. & TAYLOR, F.C. (1969): Hill Island Lake. *Geol. Surv. Can., A-Ser. Map* **1203A**.

NICHOLS, G.T., BERRY, R.F. & GREEN, D.H. (1992): Internally consistent gahnitic spinel – cordierite – garnet equilibria in the FMASHZn system: geothermobarometry and applications. *Contrib. Mineral. Petrol.* **111**, 362-377.

NIELSEN, P.A., LANGENBERG, C.W., BAADSGAARD, H. & GODFREY, J.D. (1981): Precambrian metamorphic conditions and crustal evolution, northeastern Alberta, Canada. *Precambrian Res.* **16**, 171-193.

PATIÑO DOUCE, A.E. & BEARD, J.S. (1995): Dehydration melting of biotite gneiss and quartz amphibolite from 3 to 15 kbar. *J. Petrol.* **36**, 707-738.

________, HUMPHREYS, E.D. & JOHNSTON, A.D. (1990): Anatexis and metamorphism in tectonically thickened continental crust exemplified by the Sevier hinterland, western North America. *Earth Planet. Sci. Lett.* **97**, 290-315.

________ & JOHNSTON, A.D. (1991): Phase equilibria and melt productivity in the pelitic system; implications for the origin of peraluminous granitoids and aluminous granulites. *Contrib. Mineral. Petrol.* **107**, 202-218.

PATTISON, D.R.M. & BÉGIN, N.J. (1994): Compositional maps of metamorphic orthopyroxene and garnet: evidence for a hierarchy of closure temperatures and implications for geothermometry of granulites. *J. Geol.* **12**, 387-410.

PLATT, J.P. & ENGLAND, P.C. (1994): Convective removal of lithosphere beneath mountain belts: thermal and mechanic consequences. *Am. J. Sci.* **294**, 307-336.

PLINT, H.E. & MCDONOUGH, M.R. (1995): $^{40}Ar/^{39}Ar$ and K–Ar age constraints on shear zone evolution, southern Taltson magmatic zone, northeastern Alberta. *Can. J. Earth Sci.* **32**, 281-291.

POUCHOU, J.L. & PICHOIR, F. (1985): "PAP" (phi-rho-Z) procedure for improved quantitative microanalysis. *Microbeam Anal.* **20**, 104-106.

ROSS, G.M., PARRISH, R.R., VILLENEUVE, M.E. & BOWRING, S.A. (1991): Geophysics and geochronology of the crystalline basement of the Alberta Basin, western Canada. *Can. J. Earth Sci.* **28**, 512-522.

SMITH, J.V. & BROWN, W.L. (1988): *Feldspar Minerals: Crystal Structures, Physical, Chemical and Microtextural Properties*. Springer-Verlag, New York, N.Y.

THÉRIAULT, R. (1992): Nd isotopic evolution of the Taltson Magmatic Zone, Northwest Territories, Canada: insights into early Proterozoic accretion along the western margin of the Churchill Province. *J. Geol.* **100**, 465-475.

________ (1994): Nd isotopic evidence for Protopaleozoic pre-Taltson Magmatic Zone (1.99–1.90 Ga) rifting of the western Churchill Province. *In* Alberta Basement Transects Workshop **37** (G.M. Ross, ed.). University of British Columbia, Vancouver, British Columbia (267-269).

________ & ROSS, G.M. (1991): Nd isotopic evidence for crustal recycling in the ca. 2.0 Ga subsurface of western Canada. *Can. J. Earth Sci.* **28**, 1140-1147.

THOMPSON, A.B. & CONNOLLY, J.A.D. (1995): Melting of the continental crust: some thermal and petrological constraints on anatexis in continental collision zones and other tectonic settings. *J. Geophys. Res.* **100**, 15565-15579.

THOMPSON, P.H., CULSHAW, N., BUCHANAN, J.R. & MANOJLOVIC, P. (1986): Geology of the Slave Province and Thelon tectonic zone in the Tinney Hills – Overby Lake (west half) map area, District of Mackenzie. *Geol. Surv. Can., Pap.* **86-1A**, 275-289.

TRACY, R.J. (1982): Compositional zoning and inclusion in metamorphic minerals. *In* Characterization of Metamorphism Through Mineral Equilibria (J.M. Ferry, ed.). *Rev. Mineral.* **10**, 355-397.

VAN BREEMEN, O. & ASPLER, L.B. (1994): Detrital zircon ages from Nonacho Basin, western Rae Province, Northwest Territories.*In* Radiometric Age and Isotopic Studies. *Geol. Surv. Can., Pap.* **94-1C**, 49-59.

VIELZEUF, D. & HOLLOWAY, J.R. (1988): Experimental determination of the fluid-absent melting relations in the pelitic system. Consquences for crustal differentiation. *Contrib. Mineral. Petrol.* **98**, 257-276.

WATERS, D.J. (1991): Hercynite–quartz granulites: phase relations and implications for crustal processes. *Eur. J. Mineral.* **3**, 367-386.

WELLS, P.R.A. (1980): Thermal models for the magmatic accretion and subsequent metamorphism of continental crust. *Earth Planet. Sci. Lett.* **46**, 253-265.

XU, G., WILL, T.M. & POWELL, R. (1994): A calculated petrogenetic grid for the system K_2O–FeO–MgO–Al_2O_3–SiO_2–H_2O, with particular reference to contact-metamorphosed pelites. *J. Metamorphic Geol.* **12**, 99-119.

Received February 24, 1997, revised manuscript accepted July 2, 1997.